DMD Fast Forward. Published on February 28, 2023 as DOI: 10.1124/dmd.122.000970
This article has not been copyedited and formatted. The final version may differ from this version.

Preincubation time-dependent, long-lasting inhibition of drug transporters and impact on the prediction of drug-drug interactions

Yoshitane Nozaki and Saki Izumi

Global Drug Metabolism and Pharmacokinetics, Tsukuba Research Laboratories, Eisai Co., Ltd.,

5-1-3, Tokodai, Tsukuba, Ibaraki, 300-2635, Japan (Y. N., S. I.)

DMD Fast Forward. Published on February 28, 2023 as DOI: 10.1124/dmd.122.000970
This article has not been copyedited and formatted. The final version may differ from this version.

Running Title Page

Running title: Preincubation effect on transporter inhibition potency

Corresponding author: Yoshitane Nozaki, PhD

Global Drug Metabolism and Pharmacokinetics, Tsukuba Research Laboratories, Eisai Co., Ltd.

5-1-3, Tokodai, Tsukuba, Ibaraki, 300-2635, Japan

Telephone: +81-70-2474-2916

Fax: +81-29-847-5672

E-mail: y2-nozaki@hhc.eisai.co.jp

Number of Text Pages: 61

Number of Tables: 2

Number of Figures: 6

Number of Supplemental Tables: 3

Number of words in the Abstract: 237

Number of words in the Significance Statement: 75

Number of words in the Main Test: 6118

DMD Fast Forward. Published on February 28, 2023 as DOI: 10.1124/dmd.122.000970
This article has not been copyedited and formatted. The final version may differ from this version.

Abbreviation:

AUC, area under the plasma concentration-time curve; BSP, sulphobromophthalein; CsA, cyclosporine A; CYP, cytochrome P450; DDI, drug-drug interaction; E_1S, estrone-3-sulfate; E_2G, estradiol-17β-glucuronide; EMA, European Medicines Agency; FDA, U.S. Food and Drug Administration; HBV, hepatitis B virus; HDV, hepatitis D virus; HEK293, human embryonic kidney 293; IC_{50}, half maximal inhibitory concentration; K_i, inhibition constant; $K_{p,uu}$, intracellular-to-extracellular or tissue-to-plasma unbound drug concentration ratio; LAT, L-type amino acid transporter; MATE, multidrug and toxin extrusion; MDCK, Madin-Darby canine kidney; MHLW, Ministry of Health, Labour and Welfare; NTCP, Na^+/taurocholate cotransporting polypeptide; OAT, organic anion transporter; OATP/Oatp, organic anion transporting polypeptide; OCT, organic cation transporter; SLC, solute carrier; statin, 3-hydroxy-3-methylglutaryl-CoA reductase inhibitor; TCA, taurocholic acid; TDI, time-dependent inhibition; TLC, taurolithocholic acid.

DMD Fast Forward. Published on February 28, 2023 as DOI: 10.1124/dmd.122.000970
This article has not been copyedited and formatted. The final version may differ from this version.

Abstract

Transporter-mediated drug-drug interaction (DDI) is of clinical concern, and the quantitative prediction of DDIs is an indispensable part of drug development. Cell-based inhibition assays, in which a representative probe substrate and a potential inhibitor are coincubated, are routinely performed to assess the inhibitory potential of new molecular entities on drug transporters. However, the inhibitory effect of cyclosporine A (CsA) on organic anion transporting polypeptide (OATP) 1B1 is substantially potentiated with CsA preincubation, and this effect is both long-lasting and dependent on the preincubation time. This phenomenon has also been reported with transporters other than OATP1Bs, but it is considered more prevalent among OATP1Bs and organic cation transporters. Regulatory agencies have also noted this preincubation effect and have recommend that pharmaceutical companies consider inhibitor preincubation when performing in vitro OATP1B1 and OATP1B3 inhibition studies. Although the underlying mechanisms responsible for the preincubation effect are not fully understood, a *trans*-inhibition mechanism was recently demonstrated for OATP1B1 inhibition by CsA, in which CsA inhibited OATP1B1 not only extracellularly (*cis*-inhibition), but also intracellularly (*trans*-inhibition). Furthermore, the *trans*-inhibition potency of CsA was much greater than that of *cis*-inhibition, suggesting that *trans*-inhibition might be a key driver of clinical DDIs of CsA with OATP1B substrate drugs. Although confidence in transporter-mediated DDI prediction is

DMD Fast Forward. Published on February 28, 2023 as DOI: 10.1124/dmd.122.000970
This article has not been copyedited and formatted. The final version may differ from this version.

generally considered to be low, the predictability might be further improved by incorporating the *trans*-inhibition mechanism into static and dynamic models for preincubation-dependent inhibitors of OATP1Bs and perhaps other transporters.

Significance Statement

Preincubation time-dependent, long-lasting inhibition has been observed for OATP1B1 and other solute carrier transporters in vitro. Recently, a *trans*-inhibition mechanism for the preincubation effect of CsA on OATP1B1 inhibition was identified, with the *trans*-inhibition potency being greater than that of *cis*-inhibition. The concept of *trans*-inhibition may allow us to further understand the mechanism of transporter-mediated DDIs not only for OATP1B1, but also for other transporters and to improve the accuracy and confidence of DDI predictions.

DMD Fast Forward. Published on February 28, 2023 as DOI: 10.1124/dmd.122.000970
This article has not been copyedited and formatted. The final version may differ from this version.

Introduction

In current pharmacotherapy, patients are commonly treated with multiple drugs to achieve therapeutic purposes, but the potential risk of drug-drug interactions (DDIs) demands caution. When the metabolism and/or excretion processes of a drug with a narrow therapeutic index are inhibited by concomitant medications, the increased systemic exposure of the affected drug may cause toxicities, including life-threatening adverse effects in a worst-case scenario. Indeed, severe toxicities caused by DDIs have been reported clinically (Honig et al., 1993; Diasio, 1998; Mullins et al., 1998; Bruno-Joyce et al., 2001); such toxicities can result in the withdrawal of approved drugs from the market, even if therapeutic benefits are available to some patient populations. To avoid such clinical safety issues, pharmaceutical companies characterize the DDI potentials of new molecular entities (NMEs) at various stages of drug development according to regulatory DDI guidance or guidelines (EMA, 2013; MHLW, 2018; FDA, 2020).

Recently, significant research progress has revealed that drug transporters as well as drug metabolizing enzymes, such as cytochrome P450 (CYP), are potential sites of DDIs, and an increasing number of transporter-mediated DDIs have been reported (Gessner et al., 2019). Of the transporters involved in drug pharmacokinetics (PK), P-glycoprotein (P-gp, *ABCB1*), breast cancer resistance protein (BCRP, *ABCG2*), organic anion transporting polypeptide (OATP) 1B1 (*SLCO1B1*), OATP1B3 (*SLCO1B3*), organic anion transporter (OAT) 1 (*SLC22A6*), OAT3

DMD Fast Forward. Published on February 28, 2023 as DOI: 10.1124/dmd.122.000970
This article has not been copyedited and formatted. The final version may differ from this version.

(*SLC22A8*), organic cation transporter (OCT) 1 (*SLC22A1*), OCT2 (*SLC22A2*), multidrug and toxin extrusion (MATE) 1 (*SLC47A1*), and MATE2-K (*SLC47A2*) are commonly acknowledged as being clinically relevant transporters (Giacomini et al., 2010; Yonezawa and Inui, 2011; Zamek-Gliszczynski et al., 2018). These transporters are involved in the active efflux of various drugs in the intestine and blood-brain barrier (P-gp, BCRP), hepatobiliary excretion (basolateral uptake by OATP1B1, OATP1B3, and/or OCT1 followed by active efflux by P-gp, BCRP, MATE1, and/or other efflux transporters via the canalicular membrane), or renal tubular secretion (basolateral uptake by OAT1, OAT3, and/or OCT2 followed by luminal efflux by P-gp, BCRP, MATE1, MATE2-K, and/or other efflux transporters), and the altered function of these transporters by DDIs could impact the clinical PK as well as the safety of the substrate drugs. One well-known example is the interaction of 3-hydroxy-3-methylglutaryl-CoA reductase inhibitors (statins) with cyclosporine A (CsA) (Neuvonen et al., 2006; Shitara and Sugiyama, 2006). The OATP1B-mediated hepatic uptake of statins is potently inhibited by CsA (Billington et al., 2019), resulting in increased systemic exposure to statins and a higher incidence rate of statin myotoxicity (Ballantyne et al., 2003; Link et al., 2008). Selecting drug candidates that have no or an acceptable risk of DDI before first-in-human clinical studies is the most straightforward approach to minimize such risk. To this end, drug candidates are routinely evaluated for their inhibition potency against drug transporters at nonclinical stages.

DMD Fast Forward. Published on February 28, 2023 as DOI: 10.1124/dmd.122.000970
This article has not been copyedited and formatted. The final version may differ from this version.

In conventional cell-based inhibition assays for uptake transporters, a representative probe substrate and an NME as a potential inhibitor are simultaneously added to transporter-transfected cells, and the uptake of the probe substrate is then examined for a short period of time in the presence of the inhibitor, based on the assumption that the inhibitor can inhibit transporter molecules from outside the cells (*cis*-inhibition) only. However, the examples from multiple inhibitors have demonstrated that employing a preincubation with cells prior to the conventional inhibition study can increase their inhibitory impact on certain transporters. OATP1B1 inhibition by CsA is a typical example, where the inhibitory effect of CsA on OATP1B1 was potentiated depending on the preincubation time, and the reduced OATP1B1 function slowly recovered even after the removal of CsA from the incubation buffer (Shitara and Sugiyama, 2017). This phenomenon has also been noted for other OATP1B inhibitors and other transporters (Tátrai et al., 2019).

The preincubation effect may result in an altered inhibition constant (K_i) or half maximal inhibitory concentration (IC_{50}) values compared to conventional method, and consequently can have an impact on clinical DDI risk assessments. The in vitro transporter inhibition study design should be carefully planned to reflect this. The preincubation time-dependency observed during the transporter inhibition is apparently very similar to the time-dependent inhibition (TDI) of drug metabolizing enzymes such as CYPs while a different mechanism (i.e., *trans*-inhibition)

DMD Fast Forward. Published on February 28, 2023 as DOI: 10.1124/dmd.122.000970
This article has not been copyedited and formatted. The final version may differ from this version.

was recently demonstrated for some transporter-inhibitor pairs (Lowjaga et al., 2021; Izumi et al., 2022). Although this research area is still actively evolving, in this minireview we summarized the current knowledge on the preincubation effects observed in transporter inhibition studies and discussed the potential impact on the quantitative prediction of transporter-mediated DDIs with a reference to the proposed *trans*-inhibition mechanism.

Preincubation time-dependent, long-lasting inhibition of OATP1Bs

The preincubation time-dependent, long-lasting inhibition of drug transporters was first reported by Shitara et al., who examined the inhibition of rat Oatp transporters by CsA in vitro and in vivo using sulfobromophthalein (BSP) as a probe substrate (Shitara et al., 2009). In the liver uptake index experiment, the in vivo hepatic uptake of BSP was impaired for 3 days after CsA treatment and returned to the baseline level on day 5. The unbound plasma concentration of CsA could not account for this long-lasting inhibition. They also found that the inhibitory effect of CsA on BSP uptake into primary cultured rat hepatocytes was potentiated after CsA preincubation, with an IC_{50} value of 0.126 μmol/L under the no preincubation condition and decreasing to 0.0583 and 0.0422 μmol/L after 20 and 60 minutes of preincubation with CsA, respectively. Subsequently, Amundsen and coworkers demonstrated that the inhibitory effect of CsA on human OATP1B1 was greatly potentiated by the addition of a CsA preincubation step in

DMD Fast Forward. Published on February 28, 2023 as DOI: 10.1124/dmd.122.000970
This article has not been copyedited and formatted. The final version may differ from this version.

vitro (Amundsen et al., 2010). Preincubating OATP1B1-transfected HEK293 cells with CsA for 60 minutes before the substrate (atorvastatin) and CsA coincubation potentiated the effect on OATP1B1 by a factor of 22, compared with a no-preincubation condition (IC_{50} of 0.021 and 0.47 μmol/L, respectively). These findings prompted multiple groups, including us, to investigate the preincubation effect on the OATP1B1 and OATP1B3 inhibition potency.

Currently, the following compounds have exhibited a 3-fold or greater potentiation of OATP1B1 inhibition after preincubation in vitro in at least one examination: venetoclax (fold potentiation, >258), CsA (3.2–61), nilotinib (>42), regorafenib (>24), rifampin (0.5–9.3), everolimus (2.1–8.3), pazopanib (2.7–6.7), asunaprevir (4.9), AM1 (a metabolite of CsA, 4.4), and saquinavir (3.5) (Table 1 and Supplementary Table 1). CsA, AM1, saquinavir, and venetoclax also showed a 3-fold or greater preincubation effect on OATP1B3 inhibition potency (Table 1). Rifampin is a prototypical inhibitor for OATP1Bs in vitro and in vivo, but the preincubation effect was modest, compared with that of CsA. Of note, not all inhibitors exhibited a preincubation effect (Supplementary Table 1).

In addition to the preincubation effect, substrate-dependent inhibition is also a unique characteristic of the OATP1B1 molecule, in which the inhibition potency of an inhibitor on OATP1B1 can vary greatly depending on the probe substrates used in vitro (Noe et al., 2007; Izumi et al., 2013). Using five probe substrates (E_2G [estradiol-17β-glucuronide], E_1S [estrone-

DMD Fast Forward. Published on February 28, 2023 as DOI: 10.1124/dmd.122.000970
This article has not been copyedited and formatted. The final version may differ from this version.

3-sulfate], BSP, atorvastatin, and pitavastatin), we investigated the preincubation effect of CsA on OATP1B1 (Izumi et al., 2015). A lower K_i value of CsA was given when E_2G was used as a probe substrate; however, the degree of the K_i shift was similar (3.2- to 5.1-fold) regardless of the probe substrates that were examined (Figure 1).

As reported earlier (Shitara et al., 2009), the preincubation effect was detected not only in transfected cells, but also in hepatocyte systems (Supplementary Table 2). Although the degree of potentiation was not examined, 30 minutes of preincubation with CsA inhibited the uptake of E_1S into plated human hepatocytes even after the removal of CsA from the incubation buffer (Shitara et al., 2012). In the sandwich-cultured human hepatocytes, 60 minutes of preincubation with everolimus potentiated the inhibitory effect by 3.6-fold or greater when pitavastatin and cholecystokinin octapeptide (CCK-8) were used as probe substrates for OATP1B1 and OATP1B3, respectively (Farasyn et al., 2021). A preincubation effect was also noted in monkey hepatocytes. By preincubating plated monkey hepatocytes with CsA for 60 minutes before the substrate and inhibitor coincubation, the inhibitory effect on the uptake of pitavastatin was potentiated by 3.7-fold (Ufuk et al., 2018), the degree of which was for unknown reasons weaker than that observed in cynomolgus monkey OATP1B1- and OATP1B3-transfected cells (23- and 7.7-fold, respectively) (Takahashi et al., 2016). Therefore, a preincubation effect has also been seen in in vitro hepatocyte systems, implying an in vivo relevance for nonhuman

DMD Fast Forward. Published on February 28, 2023 as DOI: 10.1124/dmd.122.000970
This article has not been copyedited and formatted. The final version may differ from this version.

primates and humans, in addition to rats (Shitara et al., 2009; Taguchi et al., 2016).

To predict the potential of NMEs to inhibit OATP1B1 and OATP1B3 in vivo, the R-value is calculated according to the static model using the in vitro K_i value as follows:

$$R = 1 + \frac{[I]}{K_i} \quad (1)$$

where [I] represents the inhibitor concentration. The latest regulatory DDI guidance and guidelines recommend the following $I_{u,in,max}$ (the maximum unbound inhibitor concentration at the inlet to the liver) for [I]:

$$I_{u,in,max} = f_p \cdot \left(I_{max} + \frac{F_a \cdot F_g \cdot k_a \cdot Dose}{Q_h \cdot R_B}\right) \quad (2)$$

where f_p is the unbound fraction in plasma, I_{max} is the maximum total plasma concentration, F_a is the fraction absorbed, F_g is the fraction of absorbed dose escaping from the intestinal metabolism, k_a is the absorption rate constant, Dose is the clinical dose of the inhibitor, Q_h is the hepatic blood flow rate (97 L/h), and R_B is the blood-to-plasma concentration ratio (Ito et al., 1998). When the calculated R-value is equal to or greater than the cut-off value (1.1, proposed by FDA and MHLW), the NME is considered a potential in vivo inhibitor of OATP1B1 or OATP1B3 that warrants further evaluation including a dynamic physiologically-based pharmacokinetic (PBPK) model analysis and/or clinical DDI study. However, the confidence in OATP1B-mediated DDI predictions based on the static and dynamic models is generally acknowledged to be relatively low, compared with that of CYP-mediated DDI predictions

DMD Fast Forward. Published on February 28, 2023 as DOI: 10.1124/dmd.122.000970
This article has not been copyedited and formatted. The final version may differ from this version.

(Yoshida et al., 2012; Vaidyanathan et al., 2016; Taskar et al., 2020). In addition to the uncertainties around the $I_{u,in,max}$ estimation, large variabilities have been observed in the reported in vitro K_i and IC_{50} values for OATP1B1 (Figure 2). Complex inhibition mechanisms such as the preincubation effect and substrate-dependency may make accurate determinations of in vitro IC_{50} and K_i values difficult, but the exact reason for the low confidence remains to be elucidated. Although the accurate prediction of OATP1B-mediated DDIs remains challenging, we would be able to reduce the risk of false-negative DDI predictions at least for preincubation effect-positive inhibitors by using lower K_i values obtained after inhibitor preincubation. Regulatory agencies have also acknowledged the preincubation effect (MHLW, 2018; FDA, 2020), and 30 minutes or longer of preincubation with NMEs is recommended for evaluating the in vitro inhibition potencies for OATP1B1 and OATP1B3 in the latest MHLW DDI guideline.

Preincubation effect observed for other transporters

In addition to OATP1B1 and OATP1B3, Tátrai and coauthors systematically examined the IC_{50} values of various compounds for OAT1, OAT3, OCT1, OCT2, MATE1, and MATE2-K in vitro with or without 3 hours of inhibitor preincubation (Tátrai et al., 2019). After giving careful consideration to the nonspecific binding of the inhibitors to labware as well as cell viability, they found that the potentiation of transporter inhibition by preincubation was

DMD Fast Forward. Published on February 28, 2023 as DOI: 10.1124/dmd.122.000970
This article has not been copyedited and formatted. The final version may differ from this version.

prevalent among OCTs and OATP1Bs, but not among OATs or MATEs. One of the most pronounced preincubation effects observed in their study was the inhibition of OCT1 by ledipasvir, with a >255-fold potentiation (Table 2).

CsA exhibited a preincubation effect not only for OATP1Bs, but also for OCT1 (Panfen et al., 2019). When metformin was used as a substate, the inhibition potency of CsA on OCT1 was increased by 50.2-fold after a 30-minute preincubation with CsA (IC_{50} of 0.43 versus 21.6 μmol/L). However, this effect greatly depended on the substrate, with only a 3.2-fold or less potentiation observed for the OCT1-mediated uptake of sumatriptan and cycloguanil (Table 2 and Supplemental Table 1). We may need to select OCT1 probe substrates carefully when evaluating the preincubation effect. For OCT2, crizotinib showed a preincubation effect (Arakawa et al., 2017). With or without crizotinib preincubation, a lower IC_{50} value of crizotinib was obtained when creatinine, rather than 1-methyl-4-phenylpyridinium (MPP^+), was used as a substrate, but the degree of potentiation after crizotinib preincubation was similar between creatinine and MPP^+ (4.6- and 3.5-fold, respectively) (Table 2).

Although information is limited for OATs and MATEs, crizotinib and imatinib showed a preincubation effect on MATE1 with a 3.1- to 3.8-fold and a 7.2-fold potentiation, respectively (Omote et al., 2018) (Table 2). Some anthraquinone derivatives from a traditional Chinese medicine showed a preincubation-dependency for the OAT1 (chrysophanol, physcion) and

DMD Fast Forward. Published on February 28, 2023 as DOI: 10.1124/dmd.122.000970
This article has not been copyedited and formatted. The final version may differ from this version.

OAT3 (emodin, aloe-emodin, chrysophanol, physcion) inhibition potencies (Ma et al., 2015).

OATP2B1 (*SLCO2B1*) is thought to play a role in the intestinal and hepatic uptake of anionic drugs, but its clinical relevance remains debatable (Zamek-Gliszczynski et al., 2022). Apple juice and (to a lesser extent) orange juice exerted a preincubation effect on OATP2B1 inhibition in vitro, which may account for the mechanism of the food-drug interaction between apple/orange juice and fexofenadine that has been observed clinically (Shirasaka et al., 2013). L-type amino acid transporter 1 (LAT1, SLC7A5) is expressed in various types of tumor cells and is thought to contribute to tumor progression by supplying essential amino acids. JPH203 was developed as an LAT1 inhibitor and exhibits a preincubation effect on LAT1 in human colon adenocarcinoma HT-29 cells, yielding a 2.9-fold potentiation after a 2-hour preincubation (Okunushi et al., 2020).

Therefore, preincubation time-dependent, long-term inhibition is not unique to OATP1Bs, but is commonly observed for SLC transporters to varying degrees. When a borderline R-value is obtained for drug candidates from a static model-based DDI prediction (Eq. 1) following a conventional coincubation method, additional testing of the preincubation effect may help to avoid false-negative predictions for non-OATP1B transporters. By using the K_i values obtained after inhibitor preincubation, the outcomes of DDI risk assessments reportedly changed from “no risk” to “risk” for OCT2 inhibition by dolutegravir, irinotecan, isavuconazole, and

DMD Fast Forward. Published on February 28, 2023 as DOI: 10.1124/dmd.122.000970
This article has not been copyedited and formatted. The final version may differ from this version.

vandetanib according to the EMA criteria (Tátrai et al., 2019). For non-OATP1B transporters, however, currently available data on the preincubation effect is limited (Supplemental Table 1). More data sets are needed to determine the need for an inhibitor preincubation step even for non-OATP1B transporters.

Trans-inhibition as an underlying mechanism for the preincubation effect of CsA on OATP1B1 inhibition

Even though this preincubation effect of transporters and metabolic enzyme-mediated TDI apparently share characteristics in common, such as (preincubation) time-dependency and long-lasting inhibition, the underlying mechanisms are considered to be different. Reactive intermediates are unlikely to be involved in the preincubation effect of transporters, due to the nature of lacking sufficient expression of metabolic enzymes with in vitro systems used in the transporter inhibition study (e.g., HEK293 cells). Very recently, a *trans*-inhibition mechanism for the preincubation effect of CsA on OATP1B1 inhibition potency was experimentally demonstrated (Izumi et al., 2022).

The intracellular CsA concentration was suggested to be a key driver of the preincubation effect on OATP1B1 observed in vitro. Shitara and coworkers spiked CsA onto either the apical or basal side of OATP1B1-transfected MDCKII cell monolayers that had been cultured on a

DMD Fast Forward. Published on February 28, 2023 as DOI: 10.1124/dmd.122.000970
This article has not been copyedited and formatted. The final version may differ from this version.

porous membrane filter. After a 1-hour preincubation, CsA was removed from the incubation buffer, and E_1S uptake was examined to evaluate the remaining transport function of OATP1B1. Although extracellular CsA was washed out to avoid *cis*-inhibition, similar degrees of OATP1B1 inhibition for almost the same intracellular CsA concentrations were detected regardless of the CsA-spiked side. No change in the protein expression levels or cellular localization of OATP1B1 was seen in the MDCKII cells after CsA preincubation (Shitara et al., 2012). These in vitro findings as well as the theoretical consideration given by the modeling and simulation analysis prompted Shitara and Sugiyama to propose *trans*-inhibition (i.e., CsA inhibits OATP1B1 molecules from the intracellular side) as a possible mechanism for the preincubation effect on OATP1B1 (Shitara and Sugiyama, 2017).

To validate the *trans*-inhibition mechanism experimentally, our group used four assay conditions to capture *cis*-, *trans*-, both *cis*- and *trans*-inhibition (*cis*+*trans*-inhibition), and long-lasting inhibition in OATP1B1-transfected HEK293 cells (Figure 3); we then tried to account for all the in vitro findings quantitatively using a cellular PK model that took both *trans*-inhibition and *cis*-inhibition into account (Figure 4) using CsA and rifampin as inhibitors (Izumi et al., 2022). As for CsA, we found that 1) incubation for 60 minutes or longer was necessary for CsA to reach a steady-state cellular uptake because of its high-affinity, high-capacity intracellular binding, possibly with cyclophilin A (the pharmacological target of CsA)

DMD Fast Forward. Published on February 28, 2023 as DOI: 10.1124/dmd.122.000970
This article has not been copyedited and formatted. The final version may differ from this version.

(Handschumacher et al., 1984); 2) CsA inhibited OATP1B1 competitively from the outside (*cis*-inhibition) and non-competitively from the inside (*trans*-inhibition) of cells; and 3) the inhibition of OATP1B1 by CsA was potentiated by a longer preincubation with CsA under the *trans*- and *cis*+*trans*-inhibition assay conditions. The preincubation time-dependent, long-lasting inhibition of OATP1B1 by CsA was well reproduced using the cellular kinetic model (Figures 4 and 5), which revealed that the *trans*-inhibition potency of CsA ($K_{i,trans}$, 0.00619 μmol/L) was 48-fold stronger than the *cis*-inhibition potency ($K_{i,cis}$, 0.297 μmol/L) for OATP1B1. In contrast, rifampin promptly reached a steady-state of uptake into HEK293 cells (within 10 minutes), showing a modest (only 2-fold) preincubation time-dependency for the potentiation of OATP1B1 inhibition. The modest effect of rifampin was also well accounted for by a cellular PK model that considered the OATP1B1-mediated active uptake of rifampin, in which the obtained $K_{i,trans}$ (1.56 μmol/L) was similar to the $K_{i,cis}$ (1.16 μmol/L). Based on these findings, we concluded that the CsA preincubation effect could be attributed to the potent *trans*-inhibition of OATP1B1 by CsA, the effect of which was potentiated as CsA accumulated intracellularly in a preincubation time-dependent manner.

In a long-lasting inhibition study, the slow and/or partial recovery of OATP1B1 transport function was observed for CsA (Figure 5E) and rifampin (Figure 5F); this recovery was also well simulated by our cellular PK model. A deeper investigation of the simulation results

DMD Fast Forward. Published on February 28, 2023 as DOI: 10.1124/dmd.122.000970
This article has not been copyedited and formatted. The final version may differ from this version.

showed that inhibitor persisting intracellularly after washing diffused into the extracellular buffer, and a new equilibrium was subsequently established between the cell and buffer compartments during incubation with an inhibitor-free buffer. Under the new equilibrium condition, the intracellular inhibitor concentration was lower than that in the first inhibitor preincubation step, but still high enough to exhibit *trans*-inhibition, resulting in the apparently slow and/or partial recovery of transport function. Thus, caution should be exercised when analyzing the recovery kinetics of transporter function in vitro.

Tátrai and coworkers also examined time profiles for cellular concentration and degree of transporter inhibition potency for some preincubation-dependent inhibitors of OATP1B1 (venetoclax and CsA) and OCT1 (ledipasvir) (Tátrai et al., 2019). The cellular concentrations and inhibition potencies of the inhibitors followed similar time-courses, suggesting that the intracellular inhibitor concentration is a determinant of the preincubation effects. Further in-depth analysis is warranted, but the *trans*-inhibition mechanism may account for at least some of the preincubation-dependent inhibitors that have been reported to date.

The *trans*-inhibition mechanism was also recently proposed as being responsible for the inhibition of Na^+/taurocholate cotransporting polypeptide (NTCP, *SLC10A1*) by taurolithocholic acid (TLC) (Lowjaga et al., 2021). NTCP is highly expressed at the basolateral membrane of human hepatocytes and is involved in the Na^+-dependent hepatic uptake of bile acids and some

DMD Fast Forward. Published on February 28, 2023 as DOI: 10.1124/dmd.122.000970
This article has not been copyedited and formatted. The final version may differ from this version.

drugs (Dawson et al., 2009; Bi et al., 2019); it is also known as an entry receptor for the hepatitis B and D viruses (HBV and HDV) (Yan et al., 2012). The preincubation of NTCP-transfected HEK293 cells with TLC followed by intensive washing (to avoid *cis*-inhibition) showed the inhibition of not only NTCP transport function, but also the binding of the myristoylated preS1 domain peptide of the large HBV surface protein, without causing any internalization or degradation of NTCP protein. The maximum inhibitory effect of TLC on NTCP transport function was attained within 1 hour of preincubation, and the effect was long-lasting for at least 8 hours after extracellular TLC washout. TLC preincubation inhibited the NTCP-mediated uptake of taurocholic acid (TCA) and dehydroepiandrosterone sulfate only when the preincubation was performed in Na^+-containing buffer, suggesting that the Na^+-dependent cellular accumulation of TLC is a prerequisite for this effect. Interestingly, TLC preincubation did not influence the NTCP-mediated uptake of TLC itself. They also confirmed that the intracellular accumulation of TLC and the degree of inhibition of NTCP transport function followed a similar time-course. Furthermore, TLC preincubation suppressed HDV infection in NTCP-transfected HepG2 cells. These data strongly support the idea that TLC is intracellularly accumulated via Na^+-dependent NTCP-mediated uptake and that the transport and receptor functions of NTCP are inhibited by TLC as a result of a *trans*-inhibition mechanism. The authors also mentioned that this *trans*-inhibition mechanism may help to

DMD Fast Forward. Published on February 28, 2023 as DOI: 10.1124/dmd.122.000970
This article has not been copyedited and formatted. The final version may differ from this version.

protect hepatocytes from the overload of toxic bile acids and could be a novel NTCP target site for potential long-acting HBV/HDV entry inhibitors.

Although the preincubation effect has been scarcely reported for ATP-binding cassette (ABC) transporters, the *trans*-inhibition mechanism was suggested for rat bile salt export pump (Bsep, ABCB11) using in vitro membrane vesicles (Stieger et al., 2000; Akita et al., 2001). Inhibitory effects of estrogen metabolite (E_2G) and sulfate-conjugated bile acids (TLC sulfate and taurochenodeoxycholic acid sulfate) on rat Bsep-mediated transport of TCA into inside-out vesicles were pronounced when rat Bsep and multidrug resistance-associated protein 2 (Mrp2) were co-expressed in the vesicles. Since the estrogen and bile acid metabolites were substrates for Mrp2, it was proposed that they exhibited a *trans*-inhibition of Bsep after accumulating into the vesicles via Mrp2. Thus, it is likely that the *trans*-inhibition mechanism is not specific to SLC transporters but can happen to ABC transporters. In the conventional inhibition studies for ABC transporters such as P-gp and BCRP, cell-based transcellular transport assays rather than vesicle assays have been commonly employed using Caco-2 or P-gp-transfected cell monolayers (LLC-PK1, MDCKII), in which relatively long substrate and inhibitor coincubation time (e.g., 45 – 180 minutes) is adopted (Bentz et al., 2013). During the coincubation period, the inhibitor can be distributed intracellularly and exhibit *trans*-inhibition in addition to *cis*-inhibition, leaving no room for preincubation effects. This may explain why the preincubation

DMD Fast Forward. Published on February 28, 2023 as DOI: 10.1124/dmd.122.000970
This article has not been copyedited and formatted. The final version may differ from this version.

effect has been infrequently reported for ABC transporters.

As shown in Table 1 and Supplementary Table 1, reported IC_{50} fold change for OATP1B1 after preincubation are highly variable in CsA (3.2–61 fold) and rifampin (0.5–9.3 fold). Although the underlying reasons remain to be clarified, the *trans*-inhibition mechanism, in addition to possible substrate-dependency, may contribute to the inter-study or inter-laboratory variability. As discussed in the ABC transporters, substrate and inhibitor coincubation time period can affect the degree of preincubation effect even for uptake transporters (Tatrai et al. 2019). Depending on the coincubation time, *trans*-inhibition in addition to *cis*-inhibition may happen under the coincubation conditions, apparently attenuating the preincubation effect. Short coincubation time should be selected if we want to see the maximum IC_{50} shift after preincubation. When a tested inhibitor is a substrate for OATP1B1 (e.g., rifampin), preincubation effect can be variable depending on the protein expression levels of OATP1B1 in the in vitro transfected cell systems used for each laboratory. Intracellular accumulation of such inhibitors is increased by higher OATP1B1 expressions, resulting in more potent *trans*-inhibition based on the buffer concentration. These assay conditions may be potential sources of the data variability.

The *trans*-inhibition mechanism has been demonstrated or suggested mainly for OATP1B1. Further studies are warranted to determine whether the *trans*-inhibition mechanism

DMD Fast Forward. Published on February 28, 2023 as DOI: 10.1124/dmd.122.000970
This article has not been copyedited and formatted. The final version may differ from this version.

is prevalent for other inhibitors and transporters. The cellular kinetic modeling that was used to study OATP1B1 inhibition by CsA and rifampin (Izumi et al., 2022) may be useful for clarifying the involvement of *trans*-inhibition. As for the mode of inhibition, noncompetitive inhibition has been demonstrated for the *trans*-inhibition of OATP1B1 by CsA, suggesting that CsA interacts with an allosteric site of the intracellular domain of OATP1B1 protein. Since *trans*-inhibition potency can be much greater (>10-fold) than that of *cis*-inhibition, as demonstrated using CsA (Figure 4), coincubation of the substrate and inhibitor might no longer be sufficient to evaluate the inhibitory potency, at least for OATP1B1, and an inhibitor preincubation step should be incorporated into inhibition assays to avoid underestimating the DDI risk.

Characteristics of preincubation-dependent inhibitors for OATP1B1

To extract key parameters that influence the OATP1B1 inhibitors preincubation effect, we compared the cellular kinetic parameters of CsA and rifampin that were obtained directly from in vitro experiments or estimated from kinetic modeling (Figure 4) (Izumi et al., 2022). Because of the high-affinity, high-capacity intracellular binding of CsA, the intracellular drug unbound fraction (f_T) of CsA (0.000254 under a linear condition) was much lower than that of rifampin (0.0311). Passive diffusion clearance (PS_{dif} in μL/min/mg protein) was similar between

DMD Fast Forward. Published on February 28, 2023 as DOI: 10.1124/dmd.122.000970
This article has not been copyedited and formatted. The final version may differ from this version.

CsA (51.3) and rifampin (52.5). The cellular distribution was driven by passive diffusion for CsA, whereas rifampin was subjected to OATP1B1-mediated active uptake in addition to passive diffusion, resulting in an intracellular-to-buffer (extracellular) unbound concentration ratio ($K_{p,uu,in\ vitro}$) of 2.25 in OATP1B1-transfected HEK293 cells. As an index for the time to reach the half maximum intracellular concentration of inhibitors after the preincubation, we employed the following $T_{1/2,max}$:

$$T_{1/2,max} = \frac{0.693 \cdot V_{cell}}{PS_{dif} \cdot f_T} \quad (3)$$

where V_{cell} is the cellular volume (2 μL/mg protein). According to Eq. 3, a longer preincubation time would be required to reach a steady-state cellular concentration for inhibitors that show low membrane permeability (PS_{dif}) and/or a low intracellular unbound fraction (f_T). Indeed, the calculated $T_{1/2,max}$ of CsA (106 minutes) was much longer than that of rifampin (0.849 minutes) because of the very low f_T value for CsA.

In an attempt to identify physicochemical descriptors that determine the preincubation effect, Tátrai and coworkers explored the correlation of physicochemical parameters with the degree of potentiation of transporter inhibition after preincubation using 30 compounds including preincubation effect-positive and -negative inhibitors for OATP1Bs and other SLC transporters (Tátrai et al., 2019). Of the seven physicochemical parameters that were examined, molecular weight, $LogD_{7.4}$, cellular K_p predicted from $LogD_{7.4}$ ($K_{p,pred}$), and the ratio of $K_{p,pred}$ to

DMD Fast Forward. Published on February 28, 2023 as DOI: 10.1124/dmd.122.000970
This article has not been copyedited and formatted. The final version may differ from this version.

apparent permeability via MDCK cell monolayers with a low efflux activity (MDCK-LE P_{app}) showed a significant correlation with the degree of potentiation while topological polar surface area, cLogP, and MDCK-LE P_{app} alone showed a weak or poor correlation. Since $K_{p,pred}$/MDCK-LE P_{app} is a parameter corresponding to $1/(PS_{dif} \cdot f_T)$ in Eq. 3, the significant correlation that was reported seems reasonable.

In addition to the slow buildup of the cellular concentration, the intrinsic potency of *trans*-inhibition is essential for inhibitors to display a preincubation effect. Since the *cis*- and *trans*-inhibition of OATP1B1 by CsA follows competitive and noncompetitive inhibition, respectively (Izumi et al., 2022), OATP1B1-mediated uptake clearance in the presence of CsA ($CL_{OATP1B1+I}$) under the *cis*+*trans*-inhibition assay condition (Figure 3) can be described as follows:

$$CL_{OATP1B1+I} = \frac{{V_{max}}/{\left(1+{f_T \cdot I_{cell}}/{K_{i,trans}}\right)}}{K_m \cdot \left(1+{I_{buffer}}/{K_{i,cis}}\right)+S} \quad (4)$$

where S, V_{max}, and K_m represent the substrate concentration, the maximum uptake velocity, and Michaelis constant, respectively. I_{cell} and I_{buffer} are the intracellular and buffer concentrations of CsA, respectively. Under the linear condition ($S << K_m$), the remaining fraction of OATP1B1 activity in the presence of CsA ($CL_{OATP1B1+I}/CL_{OATP1B1}$) can be described by the following equation:

DMD Fast Forward. Published on February 28, 2023 as DOI: 10.1124/dmd.122.000970
This article has not been copyedited and formatted. The final version may differ from this version.

$$\frac{CL_{OATP1B1+I}}{CL_{OATP1B1}} = \frac{1}{\left(1+\frac{I_{buffer}}{K_{i,cis}}\right)\cdot\left(1+\frac{f_T\cdot I_{cell}}{K_{i,trans}}\right)} \quad (5)$$

For an inhibitor that shows noncompetitive inhibition for both *cis*- and *trans*-inhibition, $CL_{OATP1B1+I}$ can be described as follows:

$$CL_{OATP1B1+I} = \frac{V_{max}\Big/\left\{\left(1+{f_T\cdot I_{cell}}\Big/{K_{i,trans}}\right)\cdot\left(1+{I_{buffer}}\Big/{K_{i,cis}}\right)\right\}}{K_m+S} \quad (6)$$

Under the linear condition ($S << K_m$), Eq. 6 can also provide Eq. 5. Thus, Eq. 5 holds true for noncompetitive inhibitors for both *cis*- and *trans*-inhibition. At a steady state after a sufficient preincubation time, the intracellular unbound concentration of the inhibitor ($f_T \cdot I_{cell}$) can be replaced by $K_{p,uu,in\ vitro} \cdot I_{buffer}$. By using the $K_{i,cis}$-to-$K_{i,trans}$ ratio (α), the following equation can be drawn from Eq. 5:

$$\frac{CL_{OATP1B1+I}}{CL_{OATP1B1}} = \frac{1}{\left(1+\frac{I_{buffer}}{K_{i,cis}}\right)\cdot\left(1+\frac{\alpha\cdot K_{p,uu,in\ vitro}\cdot I_{buffer}}{K_{i,cis}}\right)} \quad (7)$$

where $(1+I_{buffer}/K_{i,cis})$ and $(1+\alpha\cdot K_{p,uu,in\ vitro}\cdot I_{buffer}/K_{i,cis})$ represent the *cis*- and *trans*-inhibition potencies, respectively, in OATP1B1-transfected cells. Therefore, $\alpha\cdot K_{p,uu,in\ vitro}$ is a determinant of the degree of potentiation after inhibitor preincubation. The $K_{p,uu,in\ vitro}$ of CsA can be assumed to be unity because of the passive diffusion-driven cellular distribution. Meanwhile, the *trans*-inhibition potency of CsA was much stronger than that of *cis*-inhibition (α of 48.0), resulting in an $\alpha\cdot K_{p,uu,in\ vitro}$ of 48. Because of OATP1B1-mediated active uptake, the $K_{p,uu,in\ vitro}$ of rifampin was 2.25, while symmetrical *cis*- and *trans*-inhibition potency yielded an α of 0.744, resulting in a modest preincubation effect with $\alpha\cdot K_{p,uu,in\ vitro}$ value of 1.7 (Figure 4). For NTCP inhibition

DMD Fast Forward. Published on February 28, 2023 as DOI: 10.1124/dmd.122.000970
This article has not been copyedited and formatted. The final version may differ from this version.

by TLC (Lowjaga et al., 2021), a higher $K_{p,uu,in\ vitro}$ of TLC driven by Na^+-dependent NTCP uptake may contribute to the potent *trans*-inhibition.

Therefore, for preincubation-dependent inhibitors that have a *trans*-inhibition potency on OATP1B1, the time to reach a steady-state cellular concentration ($T_{1/2,max}$), the *trans*-inhibition potency relative to *cis*-inhibition (α), and the degree of the cellular accumulation of unbound inhibitor ($K_{p,uu,in\ vitro}$) are key factors of the time-dependency. Since these parameters are compound-specific, in vitro assay conditions such as the preincubation time period for reaching steady-state intracellular concentration may need to be optimized for each compound. When NMEs are tested for OATP1B1 substrate liability using the same cell systems, the time-course data on the cellular uptake may help to optimize the preincubation time for inhibition studies. According to Eq. 3, a low membrane permeability and/or strong intracellular binding contributes to a longer $T_{1/2,max}$. In addition to high-affinity, high-capacity binding to pharmacological target proteins (e.g., CsA), strong intracellular nonspecific binding of lipophilic compounds and lysosomal trapping of basic compounds could also result in long $T_{1/2,max}$ values in transfected cells. Further studies examining the cell retention mechanisms of preincubation time-dependent inhibitors are needed and may help us to understand why preincubation-dependent inhibition is most prevalent among OATP1B and OCT family transporters.

DMD Fast Forward. Published on February 28, 2023 as DOI: 10.1124/dmd.122.000970
This article has not been copyedited and formatted. The final version may differ from this version.

Clinical relevance of *trans*-inhibition mechanism to OATP1B1-mediated DDIs

To clarify the clinical relevance of the preincubation-time dependent, long-lasting inhibition of OATP1Bs, Mochizuki and coworkers performed clinical DDI studies, in which healthy volunteers orally received an OATP1B probe cocktail (pitavastatin, rosuvastatin, valsartan) 1 or 3 hours after an oral dose of CsA at 75 mg (Mochizuki et al., 2022b). Unlike in rats (Shitara et al., 2009), the inhibitory effect of CsA on OATP1Bs did not persist in humans; 1- and 3-hour dosing intervals yielded an area under the plasma concentration-time curve ratio (AUCR) of 3.46 and 2.38 for pitavastatin, and 2.16 and 1.81 for rosuvastatin, respectively. Although the exact reason for the inconsistency of long-lasting inhibition observations between human and rat results remains unknown, the different CsA blood exposure levels achieved in vivo (rats > human) and/or species differences in the metabolic clearance of CsA as well as the production of metabolite(s) that could inhibit hepatic Oatps/OATPs are potential factors. However, this clinical finding does not necessarily rule out the possibility of *trans*-inhibition mechanism in humans in vivo. Reportedly, the in vitro K_i values of CsA for OATP1B1 determined under the coincubation condition were much greater than the in vivo K_i values estimated using PBPK modeling of clinical DDIs with statins (pravastatin, pitavastatin, fluvastatin), but by applying the inhibitor preincubation method, the obtained in vitro K_i values

DMD Fast Forward. Published on February 28, 2023 as DOI: 10.1124/dmd.122.000970
This article has not been copyedited and formatted. The final version may differ from this version.

approached in vivo values (Varma et al., 2012; Yoshikado et al., 2016) (Figure 2). This analysis strongly suggested that the *trans*-inhibition of OATP1Bs by CsA, rather than *cis*-inhibition, is a major driver of the clinical DDIs with statins.

In an attempt to evaluate the impact of the *trans*-inhibition mechanism on OATP1B-mediated DDI prediction based on the static model, we have introduced the following equation from Eq. 7 to calculate the R-values of CsA and rifampin in a more mechanistic manner:

$$R = \left(1 + \frac{I}{K_{i,cis}}\right) \cdot \left(1 + \frac{K_{p,uu,in\ vivo} \cdot I}{K_{i,trans}}\right) \quad (8)$$

where $K_{p,uu,in\ vivo}$ represents the in vivo liver-to-plasma unbound concentration ratio in humans. The $K_{p,uu,in\ vivo}$ of CsA was assumed to be unity. For rifampin, the $K_{p,uu,in\ vivo}$ of 3.3 was reported previously (Chu et al., 2015). Although quantitative prediction of $K_{p,uu,in\ vivo}$ values is still a big challenge for the compounds that are subjected to active transport, several in vitro approaches using hepatocyte suspension have been proposed, including the initial uptake method (Yabe et al., 2011), the homogenization method (Riccardi et al., 2019), and the temperature method (Shitara et al., 2013; Izumi et al., 2017). The $K_{i,cis}$ value can be directly obtained from the coincubation (*cis*-inhibition) experiment in vitro. The apparent K_i value determined under the *cis*+*trans*-inhibition condition ($K_{i,app,cis+trans}$) corresponds to the inhibitor concentration in buffer (I_{buffer}) that yielded 50% inhibition of OATP1B1 in Eq. 7; thus, $K_{i,tarns}$ can be estimated from the following equation:

DMD Fast Forward. Published on February 28, 2023 as DOI: 10.1124/dmd.122.000970
This article has not been copyedited and formatted. The final version may differ from this version.

$$K_{i,trans} = \frac{K_{i,cis}+K_{i,app,cis+trans}}{K_{i,cis}-K_{i,app,cis+trans}} \cdot K_{p,uu,in\ vitro} \cdot K_{i,app,cis+trans} \quad (9)$$

By using this equation, we can experimentally estimate $K_{i,trans}$ values, without cellular kinetic modeling. When there is no evidence of OATP1B1-mediated accumulation of NMEs into transfected cells, the $K_{p,uu,in\ vitro}$ can be assumed to be unity.

To see the impact of the *trans*-inhibition mechanism on OATP1B1-mediated DDI prediction, the R-values of CsA and rifampin were calculated using static models and compared with the clinical AUCR values of OATP1B substrate drugs (Figure 6 and Supplemental Table 3). In this preliminary analysis, three different methods were used for the R-value calculations: Method 1, $R = (1 + I_{u,in,max}/K_{i,cis})$; Method 2, $R = 1 + (I_{u,in,max}/K_{i,app,cis+trans})$; and Method 3, $R = (1 + I_{u,in,max}/K_{i,cis})\cdot(1 + K_{p,uu,in\ vivo}\cdot I_{u,in,max}/K_{i,trans})$. Method 2 is recommended for OATP1B1 and OATP1B3 in regulatory guidance and guidelines (MHLW, 2018; FDA, 2020). For applying Method 3, $K_{i,trans}$ values need to be estimated following Eq. 9, but $K_{p,uu,in\ vitro}$ values of CsA and rifampin were not determined in previous studies. Thus, the $K_{p,uu,in\ vitro}$ values of 1 for CsA and 2.2 for rifampin, which were estimated in our study (Figure 4), were used for calculating the $K_{i,trans}$ values in this preliminary analysis (Supplemental Table 3).

For CsA, the consideration of *cis*-inhibition only (Method 1) substantially underestimated the AUCR, in which 6 out of 11 cases were false negatives; however, the prediction ability was greatly improved using Methods 2 or 3 with minimal false-negative

DMD Fast Forward. Published on February 28, 2023 as DOI: 10.1124/dmd.122.000970
This article has not been copyedited and formatted. The final version may differ from this version.

predictions (only 1 false negative out of 11 cases). Since Methods 2 and 3 gave similar R-values for CsA, incorporating $K_{i,app,cis+trans}$ values into Eq. 1 (Method 2) seems to be a practical approach for assessing DDI risk (Figure 6A). Rifampin showed a modest preincubation effect in vitro, and it was judged to be a potential in vivo inhibitor of OATP1B1 (R-value ≥ 1.1) regardless of the prediction methods. The highest R-values were obtained using Method 3, which took the *trans*-inhibition mechanism as well as the active intracellular accumulation of rifampin ($K_{p,uu,in\ vivo}$) into consideration (Figure 6B). For inhibitors that are expected to be actively accumulated in human hepatocytes in vivo ($K_{p,uu,\ in\ vivo}$ >1), Method 3 may be a better approach than Method 2 for avoiding false-negative predictions.

This preliminary analysis suggested that for inhibitors that display a considerable preincubation effect on OATP1B1 in vitro (e.g., CsA), assessing *cis*-inhibition only might be insufficient for DDI prediction. The incorporation of $K_{i,app,cis+trans}$ values obtained by inhibitor preincubation followed by substrate and inhibitor coincubation into Eq. 1 is considered a reasonable approach for DDI risk assessment. A more mechanistic model (Method 3) was not necessary, at least for CsA or rifampin, from the perspective of avoiding false-negative predictions. However, this preliminary analysis was made based on a very limited data set. A comprehensive analysis using a more diverse compound set is needed to determine whether Method 2 consistently yields a good performance for OATP1B-mediated DDI predictions for

DMD Fast Forward. Published on February 28, 2023 as DOI: 10.1124/dmd.122.000970
This article has not been copyedited and formatted. The final version may differ from this version.

preincubation-dependent inhibitors and whether the current regulatory cut-off value (1.1) is appropriate for this approach. In addition to the static model, a dynamic PBPK model analysis is also an important element in determining the need for clinical DDI studies, but the *trans*-inhibition mechanism is typically not considered. PBPK models that incorporate *trans*-inhibition as well as *cis*-inhibition mechanisms should be developed, as this may further improve the predictability of OATP1B-mediated DDIs with preincubation-dependent inhibitors such as CsA. Most recently, it was suggested that in vivo K_i values of CsA and rifampin given by PBPK model analysis of clinical DDI data could be lower than in vitro K_i values experimentally obtained after preincubation (Mochizuki et al., 2022a; Yoshikado et al., 2022). There are still uncertainties in the in vitro-in vivo translatability of K_i values for OATP1Bs. Until the underlying mechanisms or reasons are fully clarified, endogenous biomarker-informed PBPK modeling approach would be one of the practical and effective approaches to quantitatively predict OATP1B-mediated clinical DDIs (Yoshikado et al., 2018; Kimoto et al., 2022).

Conclusions

Since the preincubation time-dependent, long-lasting inhibition of Oatp/OATP by CsA was first reported, this phenomenon has been observed for other OATP inhibitors as well as

DMD Fast Forward. Published on February 28, 2023 as DOI: 10.1124/dmd.122.000970
This article has not been copyedited and formatted. The final version may differ from this version.

other SLC transporters. The inhibitory effect on drug transporters can be substantially potentiated by adding an inhibitor preincubation step to the conventional coincubation method, potentially impacting the outcome of the DDI prediction. Regulatory agencies have also noted this effect, and the inhibitor preincubation method is mentioned or recommended for OATP1B1 and OATP1B3 inhibition studies in the latest DDI guidance and guidelines. Although the underlying mechanism for the preincubation effect has not been fully elucidated, the *trans*-inhibition mechanism was recently confirmed to account for OATP1B1 inhibition by CsA, and the same mechanism has been implicated for other inhibitors and transporters (e.g., NTCP inhibition by TLC). By incorporating the *trans*-inhibition mechanism into static and dynamic models, the accuracy and confidence of DDI prediction may be further improved for drug transporters like OATP1Bs and beyond, contributing to the delivery of safer drugs to patients.

DMD Fast Forward. Published on February 28, 2023 as DOI: 10.1124/dmd.122.000970
This article has not been copyedited and formatted. The final version may differ from this version.

Acknowledgments

We would like to thank Professor Yuichi Sugiyama (Josai International University) for his kind guidance and close support. Sugiyama-sensei has tackled any issues in a positive manner, and his students and trainees including us have been encouraged by such a positive attitude and his enthusiasm for science and education. We hope that he could continue to show a strong leadership in the transporter research field and enjoy science. We also thank Dr. Rongrong Jiang (Eisai Inc.) for reviewing this manuscript and giving a lot of valuable advice.

DMD Fast Forward. Published on February 28, 2023 as DOI: 10.1124/dmd.122.000970
This article has not been copyedited and formatted. The final version may differ from this version.

Data Availability Statement

The authors declare that all the data supporting the findings of this study are available within the paper and its Supplemental Data.

DMD Fast Forward. Published on February 28, 2023 as DOI: 10.1124/dmd.122.000970
This article has not been copyedited and formatted. The final version may differ from this version.

Authorship Contribution

Wrote or contributed to the writing of the manuscript: Nozaki, Izumi

DMD Fast Forward. Published on February 28, 2023 as DOI: 10.1124/dmd.122.000970
This article has not been copyedited and formatted. The final version may differ from this version.

References

Akita H, Suzuki H, Ito K, Kinoshita S, Sato N, Takikawa H, and Sugiyama Y (2001) Characterization of bile acid transport mediated by multidrug resistance associated protein 2 and bile salt export pump. *Biochim Biophys Acta* **1511:**7-16.

Amundsen R, Christensen H, Zabihyan B, and Asberg A (2010) Cyclosporine A, but not tacrolimus, shows relevant inhibition of organic anion-transporting protein 1B1-mediated transport of atorvastatin. *Drug Metab Dispos* **38:**1499-1504.

Arakawa H, Omote S, and Tamai I (2017) Inhibitory Effect of Crizotinib on Creatinine Uptake by Renal Secretory Transporter OCT2. *J Pharm Sci* **106:**2899-2903.

Ballantyne CM, Corsini A, Davidson MH, Holdaas H, Jacobson TA, Leitersdorf E, März W, Reckless JP, and Stein EA (2003) Risk for myopathy with statin therapy in high-risk patients. *Arch Intern Med* **163:**553-564.

Bentz J, O'Connor MP, Bednarczyk D, Coleman J, Lee C, Palm J, Pak YA, Perloff ES, Reyner E, Balimane P, Brännström M, Chu X, Funk C, Guo A, Hanna I, Herédi-Szabó K, Hillgren K, Li L, Hollnack-Pusch E, Jamei M, Lin X, Mason AK, Neuhoff S, Patel A, Podila L, Plise E, Rajaraman G, Salphati L, Sands E, Taub ME, Taur JS, Weitz D, Wortelboer HM, Xia CQ, Xiao G, Yabut J, Yamagata T, Zhang L, and Ellens H (2013) Variability in P-glycoprotein inhibitory potency (IC_{50}) using various in vitro experimental systems:

implications for universal digoxin drug-drug interaction risk assessment decision criteria. *Drug Metab Dispos* **41:**1347-1366.

Bi YA, Costales C, Mathialagan S, West M, Eatemadpour S, Lazzaro S, Tylaska L, Scialis R, Zhang H, Umland J, Kimoto E, Tess DA, Feng B, Tremaine LM, Varma MVS, and Rodrigues AD (2019) Quantitative Contribution of Six Major Transporters to the Hepatic Uptake of Drugs: "SLC-Phenotyping" Using Primary Human Hepatocytes. *J Pharmacol Exp Ther* **370:**72-83.

Billington S, Shoner S, Lee S, Clark-Snustad K, Pennington M, Lewis D, Muzi M, Rene S, Lee J, Nguyen TB, Kumar V, Ishida K, Chen L, Chu X, Lai Y, Salphati L, Hop C, Xiao G, Liao M, and Unadkat JD (2019) Positron Emission Tomography Imaging of [(11) C]Rosuvastatin Hepatic Concentrations and Hepatobiliary Transport in Humans in the Absence and Presence of Cyclosporin A. *Clin Pharmacol Ther* **106:**1056-1066.

Bruno-Joyce J, Dugas JM, and MacCausland OE (2001) Cerivastatin and gemfibrozil-associated rhabdomyolysis. *Ann Pharmacother* **35:**1016-1019.

Chu X, Shih SJ, Shaw R, Hentze H, Chan GH, Owens K, Wang S, Cai X, Newton D, Castro-Perez J, Salituro G, Palamanda J, Fernandis A, Ng CK, Liaw A, Savage MJ, and Evers R (2015) Evaluation of cynomolgus monkeys for the identification of endogenous biomarkers for hepatic transporter inhibition and as a translatable model to predict

pharmacokinetic interactions with statins in humans. *Drug Metab Dispos* **43:**851-863.

Dawson PA, Lan T, and Rao A (2009) Bile acid transporters. *J Lipid Res* **50:**2340-2357.

Diasio RB (1998) Sorivudine and 5-fluorouracil; a clinically significant drug-drug interaction due to inhibition of dihydropyrimidine dehydrogenase. *Br J Clin Pharmacol* **46:**1-4.

EMA (2013) Guideline on the Investigation of Drug Interactions, European Medicines Agency (EMA).

Farasyn T, Pahwa S, Xu C, and Yue W (2021) Pre-incubation with OATP1B1 and OATP1B3 inhibitors potentiates inhibitory effects in physiologically relevant sandwich-cultured primary human hepatocytes. *Eur J Pharm Sci* **165:**105951.

FDA US (2020) Guidance for Industry. In Vitro Drug Interaction Studies - Cytochrome P450 Enzyme- and Transporter-Mediated Drug Interactions, Food and Drug Administration (FDA).

Furihata T, Matsumoto S, Fu Z, Tsubota A, Sun Y, Matsumoto S, Kobayashi K, and Chiba K (2014) Different interaction profiles of direct-acting anti-hepatitis C virus agents with human organic anion transporting polypeptides. *Antimicrob Agents Chemother* **58:**4555-4564.

Gertz M, Cartwright CM, Hobbs MJ, Kenworthy KE, Rowland M, Houston JB, and Galetin A (2013) Cyclosporine inhibition of hepatic and intestinal CYP3A4, uptake and efflux

transporters: application of PBPK modeling in the assessment of drug-drug interaction potential. *Pharm Res* **30:**761-780.

Gessner A, König J, and Fromm MF (2019) Clinical Aspects of Transporter-Mediated Drug-Drug Interactions. *Clin Pharmacol Ther* **105:**1386-1394.

Giacomini KM, Huang SM, Tweedie DJ, Benet LZ, Brouwer KL, Chu X, Dahlin A, Evers R, Fischer V, Hillgren KM, Hoffmaster KA, Ishikawa T, Keppler D, Kim RB, Lee CA, Niemi M, Polli JW, Sugiyama Y, Swaan PW, Ware JA, Wright SH, Yee SW, Zamek-Gliszczynski MJ, and Zhang L (2010) Membrane transporters in drug development. *Nat Rev Drug Discov* **9:**215-236.

Handschumacher RE, Harding MW, Rice J, Drugge RJ, and Speicher DW (1984) Cyclophilin: a specific cytosolic binding protein for cyclosporin A. *Science* **226:**544-547.

Honig PK, Wortham DC, Zamani K, Conner DP, Mullin JC, and Cantilena LR (1993) Terfenadine-ketoconazole interaction. Pharmacokinetic and electrocardiographic consequences. *Jama* **269:**1513-1518.

Ito K, Iwatsubo T, Kanamitsu S, Ueda K, Suzuki H, and Sugiyama Y (1998) Prediction of pharmacokinetic alterations caused by drug-drug interactions: metabolic interaction in the liver. *Pharmacol Rev* **50:**387-412.

Izumi S, Nozaki Y, Komori T, Maeda K, Takenaka O, Kusano K, Yoshimura T, Kusuhara H, and

Sugiyama Y (2013) Substrate-dependent inhibition of organic anion transporting polypeptide 1B1: comparative analysis with prototypical probe substrates estradiol-17beta-glucuronide, estrone-3-sulfate, and sulfobromophthalein. *Drug Metab Dispos* **41:**1859-1866.

Izumi S, Nozaki Y, Komori T, Takenaka O, Maeda K, Kusuhara H, and Sugiyama Y (2017) Comparison of the Predictability of Human Hepatic Clearance for Organic Anion Transporting Polypeptide Substrate Drugs Between Different In Vitro-In Vivo Extrapolation Approaches. *J Pharm Sci* **106:**2678-2687.

Izumi S, Nozaki Y, Lee W, and Sugiyama Y (2022) Experimental and Modeling Evidence Supporting the Trans-Inhibition Mechanism for Preincubation Time-Dependent, Long-Lasting Inhibition of Organic Anion Transporting Polypeptide 1B1 by Cyclosporine A. *Drug Metab Dispos* **50:**541-551.

Izumi S, Nozaki Y, Maeda K, Komori T, Takenaka O, Kusuhara H, and Sugiyama Y (2015) Investigation of the impact of substrate selection on in vitro organic anion transporting polypeptide 1B1 inhibition profiles for the prediction of drug-drug interactions. *Drug Metab Dispos* **43:**235-247.

Kimoto E, Costales C, West MA, Bi YA, Vourvahis M, David Rodrigues A, and Varma MVS (2022) Biomarker-Informed Model-Based Risk Assessment of Organic Anion

Transporting Polypeptide 1B Mediated Drug-Drug Interactions. *Clin Pharmacol Ther* **111:**404-415.

Link E, Parish S, Armitage J, Bowman L, Heath S, Matsuda F, Gut I, Lathrop M, and Collins R (2008) SLCO1B1 variants and statin-induced myopathy--a genomewide study. *N Engl J Med* **359:**789-799.

Lowjaga K, Kirstgen M, Müller SF, Goldmann N, Lehmann F, Glebe D, and Geyer J (2021) Long-term trans-inhibition of the hepatitis B and D virus receptor NTCP by taurolithocholic acid. *Am J Physiol Gastrointest Liver Physiol* **320:**G66-g80.

Ma L, Qin Y, Shen Z, Hu H, Zhou H, Yu L, Jiang H, and Zeng S (2015) Time-Dependent Inhibition of hOAT1 and hOAT3 by Anthraquinones. *Biol Pharm Bull* **38:**992-995.

MHLW (2018) Guideline on drug interaction for drug development and appropriate provision of information, Japanese Ministry of Health, Labor and Welfare (MHLW).

Mochizuki T, Aoki Y, Yoshikado T, Yoshida K, Lai Y, Hirabayashi H, Yamaura Y, Rockich K, Taskar K, Takashima T, Chu X, Zamek-Gliszczynski MJ, Mao J, Maeda K, Furihata K, Sugiyama Y, and Kusuhara H (2022a) Physiologically-based pharmacokinetic model-based translation of OATP1B-mediated drug-drug interactions from coproporphyrin I to probe drugs. *Clin Transl Sci* **15:**1519-1531.

Mochizuki T, Zamek-Gliszczynski MJ, Yoshida K, Mao J, Taskar K, Hirabayashi H, Chu X, Lai

Y, Takashima T, Rockich K, Yamaura Y, Fujiwara K, Mizuno T, Maeda K, Furihata K, Sugiyama Y, and Kusuhara H (2022b) Effect of Cyclosporin A and Impact of Dose Staggering on OATP1B1/1B3 Endogenous Substrates and Drug Probes for Assessing Clinical Drug Interactions. *Clin Pharmacol Ther* **111:**1315-1323.

Mullins ME, Horowitz BZ, Linden DH, Smith GW, Norton RL, and Stump J (1998) Life-threatening interaction of mibefradil and beta-blockers with dihydropyridine calcium channel blockers. *Jama* **280:**157-158.

Neuvonen PJ, Niemi M, and Backman JT (2006) Drug interactions with lipid-lowering drugs: mechanisms and clinical relevance. *Clin Pharmacol Ther* **80:**565-581.

Noe J, Portmann R, Brun ME, and Funk C (2007) Substrate-dependent drug-drug interactions between gemfibrozil, fluvastatin and other organic anion-transporting peptide (OATP) substrates on OATP1B1, OATP2B1, and OATP1B3. *Drug Metab Dispos* **35:**1308-1314.

Okunushi K, Furihata T, Morio H, Muto Y, Higuchi K, Kaneko M, Otsuka Y, Ohno Y, Watanabe Y, Reien Y, Nakagawa K, Sakamoto S, Wakashin H, Shimojo N, and Anzai N (2020) JPH203, a newly developed anti-cancer drug, shows a preincubation inhibitory effect on L-type amino acid transporter 1 function. *J Pharmacol Sci* **144:**16-22.

Omote S, Matsuoka N, Arakawa H, Nakanishi T, and Tamai I (2018) Effect of tyrosine kinase inhibitors on renal handling of creatinine by MATE1. *Sci Rep* **8:**9237.

Panfen E, Chen W, Zhang Y, Sinz M, Marathe P, Gan J, and Shen H (2019) Enhanced and Persistent Inhibition of Organic Cation Transporter 1 Activity by Preincubation of Cyclosporine A. *Drug Metab Dispos* **47:**1352-1360.

Park JE, Shitara Y, Lee W, Morita S, Sahi J, Toshimoto K, and Sugiyama Y (2021) Improved Prediction of the Drug-Drug Interactions of Pemafibrate Caused by Cyclosporine A and Rifampicin via PBPK Modeling: Consideration of the Albumin-Mediated Hepatic Uptake of Pemafibrate and Inhibition Constants With Preincubation Against OATP1B. *J Pharm Sci* **110:**517-528.

Riccardi KA, Tess DA, Lin J, Patel R, Ryu S, Atkinson K, Di L, and Li R (2019) A Novel Unified Approach to Predict Human Hepatic Clearance for Both Enzyme- and Transporter-Mediated Mechanisms Using Suspended Human Hepatocytes. *Drug Metab Dispos* **47:**484-492.

Shirasaka Y, Shichiri M, Murata Y, Mori T, Nakanishi T, and Tamai I (2013) Long-lasting inhibitory effect of apple and orange juices, but not grapefruit juice, on OATP2B1-mediated drug absorption. *Drug Metab Dispos* **41:**615-621.

Shitara Y, Maeda K, Ikejiri K, Yoshida K, Horie T, and Sugiyama Y (2013) Clinical significance of organic anion transporting polypeptides (OATPs) in drug disposition: their roles in hepatic clearance and intestinal absorption. *Biopharm Drug Dispos* **34:**45-78.

Shitara Y, Nagamatsu Y, Wada S, Sugiyama Y, and Horie T (2009) Long-lasting inhibition of the transporter-mediated hepatic uptake of sulfobromophthalein by cyclosporin a in rats. *Drug Metab Dispos* **37:**1172-1178.

Shitara Y and Sugiyama Y (2006) Pharmacokinetic and pharmacodynamic alterations of 3-hydroxy-3-methylglutaryl coenzyme A (HMG-CoA) reductase inhibitors: drug-drug interactions and interindividual differences in transporter and metabolic enzyme functions. *Pharmacol Ther* **112:**71-105.

Shitara Y and Sugiyama Y (2017) Preincubation-dependent and long-lasting inhibition of organic anion transporting polypeptide (OATP) and its impact on drug-drug interactions. *Pharmacol Ther* **177:**67-80.

Shitara Y, Takeuchi K, Nagamatsu Y, Wada S, Sugiyama Y, and Horie T (2012) Long-lasting inhibitory effects of cyclosporin A, but not tacrolimus, on OATP1B1- and OATP1B3-mediated uptake. *Drug Metab Pharmacokinet* **27:**368-378.

Stieger B, Fattinger K, Madon J, Kullak-Ublick GA, and Meier PJ (2000) Drug- and estrogen-induced cholestasis through inhibition of the hepatocellular bile salt export pump (Bsep) of rat liver. *Gastroenterology* **118:**422-430.

Taguchi T, Masuo Y, Futatsugi A, and Kato Y (2020) Static Model-Based Assessment of OATP1B1-Mediated Drug Interactions with Preincubation-Dependent Inhibitors Based

on Inactivation and Recovery Kinetics. *Drug Metab Dispos* **48:**750-758.

Taguchi T, Masuo Y, Kogi T, Nakamichi N, and Kato Y (2016) Characterization of Long-Lasting Oatp Inhibition by Typical Inhibitor Cyclosporine A and In Vitro-In Vivo Discrepancy in Its Drug Interaction Potential in Rats. *J Pharm Sci* **105:**2231-2239.

Taguchi T, Masuo Y, Sakai Y, and Kato Y (2019) Short-lasting inhibition of hepatic uptake transporter OATP1B1 by tyrosine kinase inhibitor pazopanib. *Drug Metab Pharmacokinet* **34:**372-379.

Takahashi T, Ohtsuka T, Uno Y, Utoh M, Yamazaki H, and Kume T (2016) Pre-incubation with cyclosporine A potentiates its inhibitory effects on pitavastatin uptake mediated by recombinantly expressed cynomolgus monkey hepatic organic anion transporting polypeptide. *Biopharm Drug Dispos* **37:**479-490.

Taskar KS, Pilla Reddy V, Burt H, Posada MM, Varma M, Zheng M, Ullah M, Emami Riedmaier A, Umehara KI, Snoeys J, Nakakariya M, Chu X, Beneton M, Chen Y, Huth F, Narayanan R, Mukherjee D, Dixit V, Sugiyama Y, and Neuhoff S (2020) Physiologically-Based Pharmacokinetic Models for Evaluating Membrane Transporter Mediated Drug-Drug Interactions: Current Capabilities, Case Studies, Future Opportunities, and Recommendations. *Clin Pharmacol Ther* **107:**1082-1115.

Tátrai P, Schweigler P, Poller B, Domange N, de Wilde R, Hanna I, Gáborik Z, and Huth F

(2019) A Systematic In Vitro Investigation of the Inhibitor Preincubation Effect on Multiple Classes of Clinically Relevant Transporters. *Drug Metab Dispos* **47:**768-778.

Ufuk A, Kosa RE, Gao H, Bi YA, Modi S, Gates D, Rodrigues AD, Tremaine LM, Varma MVS, Houston JB, and Galetin A (2018) In Vitro-In Vivo Extrapolation of OATP1B-Mediated Drug-Drug Interactions in Cynomolgus Monkey. *J Pharmacol Exp Ther* **365:**688-699.

Vaidyanathan J, Yoshida K, Arya V, and Zhang L (2016) Comparing Various In Vitro Prediction Criteria to Assess the Potential of a New Molecular Entity to Inhibit Organic Anion Transporting Polypeptide 1B1. *J Clin Pharmacol* **56 Suppl 7:**S59-72.

Varma MV, Lai Y, Feng B, Litchfield J, Goosen TC, and Bergman A (2012) Physiologically based modeling of pravastatin transporter-mediated hepatobiliary disposition and drug-drug interactions. *Pharm Res* **29:**2860-2873.

Yabe Y, Galetin A, and Houston JB (2011) Kinetic characterization of rat hepatic uptake of 16 actively transported drugs. *Drug Metab Dispos* **39:**1808-1814.

Yan H, Zhong G, Xu G, He W, Jing Z, Gao Z, Huang Y, Qi Y, Peng B, Wang H, Fu L, Song M, Chen P, Gao W, Ren B, Sun Y, Cai T, Feng X, Sui J, and Li W (2012) Sodium taurocholate cotransporting polypeptide is a functional receptor for human hepatitis B and D virus. *Elife* **3**.

Yonezawa A and Inui K (2011) Importance of the multidrug and toxin extrusion

MATE/SLC47A family to pharmacokinetics, pharmacodynamics/toxicodynamics and pharmacogenomics. *Br J Pharmacol* **164:**1817-1825.

Yoshida K, Maeda K, and Sugiyama Y (2012) Transporter-mediated drug--drug interactions involving OATP substrates: predictions based on in vitro inhibition studies. *Clin Pharmacol Ther* **91:**1053-1064.

Yoshikado T, Aoki Y, Mochizuki T, Rodrigues AD, Chiba K, Kusuhara H, and Sugiyama Y (2022) Cluster Gauss-Newton method analyses of PBPK model parameter combinations of coproporphyrin-I based on OATP1B-mediated rifampicin interaction studies. *CPT Pharmacometrics Syst Pharmacol* **11:**1341-1357.

Yoshikado T, Toshimoto K, Maeda K, Kusuhara H, Kimoto E, Rodrigues AD, Chiba K, and Sugiyama Y (2018) PBPK Modeling of Coproporphyrin I as an Endogenous Biomarker for Drug Interactions Involving Inhibition of Hepatic OATP1B1 and OATP1B3. *CPT Pharmacometrics Syst Pharmacol* **7:**739-747.

Yoshikado T, Yoshida K, Kotani N, Nakada T, Asaumi R, Toshimoto K, Maeda K, Kusuhara H, and Sugiyama Y (2016) Quantitative Analyses of Hepatic OATP-Mediated Interactions Between Statins and Inhibitors Using PBPK Modeling With a Parameter Optimization Method. *Clin Pharmacol Ther* **100:**513-523.

Zamek-Gliszczynski MJ, Giacomini KM, and Zhang L (2018) Emerging Clinical Importance of

Hepatic Organic Cation Transporter 1 (OCT1) in Drug Pharmacokinetics, Dynamics, Pharmacogenetic Variability, and Drug Interactions. *Clin Pharmacol Ther* **103:**758-760.

Zamek-Gliszczynski MJ, Sangha V, Shen H, Feng B, Wittwer MB, Varma MVS, Liang X, Sugiyama Y, Zhang L, and Bendayan R (2022) Transporters in Drug Development: International Transporter Consortium Update on Emerging Transporters of Clinical Importance. *Clin Pharmacol Ther* **112:**485-500.

Footnote

This work received no external funding. The authors declare that they have no actual or perceived conflicts of interest with the contents of this article.

DMD Fast Forward. Published on February 28, 2023 as DOI: 10.1124/dmd.122.000970
This article has not been copyedited and formatted. The final version may differ from this version.

Legends for Figures

Figure 1 Preincubation effect of CsA on OATP1B1 inhibition potency in vitro. CsA and a probe substrate, (A) [^{3}H]E_2G (0.1 μmol/L), (B) [^{3}H]E_1S (0.01 μmol/L), (C) [^{3}H]BSP (0.01 μmol/L), (D) pitavastatin (0.1 μmol/L), or (E) atorvastatin (0.1 μmol/L), were coincubated with OATP1B1-transfected HEK293 cells after 1-hour preincubation with (open squares) or without (open triangles) CsA. As a reference, cells were coincubated with CsA and a probe substrate without the preincubation step (closed circles). Thick, thin, and dashed lines represent fitted lines for coincubation of CsA and a probe substrate without preincubation, coincubation after 1-hour preincubation without CsA, and coincubation after 1-hour preincubation with CsA, respectively. Each point represents the mean ± SD (n = 3). Reproduced from Izumi S, Nozaki Y, Maeda K, Komori T, Takenaka O, Kusuhara H, and Sugiyama Y (2015) Investigation of the impact of substrate selection on in vitro organic anion transporting polypeptide 1B1 inhibition profiles for the prediction of drug-drug interactions. *Drug Metab Dispos* **43**:235-247.

Figure 2 Reported in vitro and in vivo IC_{50} or K_i values of CsA on OATP1B1. The IC_{50} or K_i values of CsA on OATP1B1 determined in vitro and in vivo were collected from the literature and plotted. In vitro inhibitory effect of CsA on OATP1B1 was determined by substrate and inhibitor coincubation without (*cis*-inhibition) and with (*cis*+*trans*-inhibition) CsA

DMD Fast Forward. Published on February 28, 2023 as DOI: 10.1124/dmd.122.000970
This article has not been copyedited and formatted. The final version may differ from this version.

preincubation (for 30 minutes or longer) using atorvastatin, BSP, E_2G, E_1S, pemafibrate, pitavastatin, rosuvastatin, fluvastatin, or pravastatin as a probe substrate (Amundsen et al., 2010; Gertz et al., 2013; Izumi et al., 2015; Taguchi et al., 2019; Tátrai et al., 2019; Taguchi et al., 2020; Park et al., 2021). The in vivo K_i values of CsA, which were able to reproduce clinical DDIs with statis, were previously estimated using PBPK modeling (Varma et al., 2012; Yoshikado et al., 2016).

Figure 3 Inhibition assay conditions to demonstrate *cis*- and *trans*-inhibition mechanisms for OATP1B1. In the *cis*-inhibition assay, a substrate and an inhibitor were coincubated without inhibitor preincubation. Since the cellular distribution of the inhibitor is minimal, OATP1B1 can be inhibited only from the outside of cells (*cis*-inhibition). In the *trans*-inhibition assay, cells were preincubated with an inhibitor. After washing cells, the uptake of the probe substrate was examined in the absence of the inhibitor. The inhibitor can inhibit OATP1B1 only from the inside of cells (*trans*-inhibition). In the *cis*+*trans*-inhibition assay, the assay flow was consistent with that of *trans*-inhibition, except for coincubation of the probe substrate and inhibitor after the inhibitor preincubation step. The inhibitor can inhibit OATP1B1 from both outside (*cis*-inhibition) and inside (*trans*-inhibition) of cells. In the long-lasting inhibition assay, cells were preincubated with an inhibitor for designated time period, followed by washout and incubation

DMD Fast Forward. Published on February 28, 2023 as DOI: 10.1124/dmd.122.000970
This article has not been copyedited and formatted. The final version may differ from this version.

with fresh buffer at 37°C. At the designated times, cells were washed again and the uptake of a probe substrate was examined in the absence of the inhibitor to monitor the recovery of OATP1B1 activity. Reproduced from Izumi S, Nozaki Y, Lee W, and Sugiyama Y (2022) Experimental and Modeling Evidence Supporting the Trans-Inhibition Mechanism for Preincubation Time-Dependent, Long-Lasting Inhibition of Organic Anion Transporting Polypeptide 1B1 by Cyclosporine A. *Drug Metab Dispos* **50**:541-551.

Figure 4 Diagram depicting *cis*- and *trans*-inhibition of OATP1B1 in vitro and cellular PK parameters of CsA and rifampin. In this model, an inhibitor in buffer (I_{buffer}) enters cells by passive diffusion (PS_{dif}) with or without OATP1B1-mediated active uptake (PS_{act}), and inhibits OATP1B1 from both outside (*cis*-inhibition) and inside (*trans*-inhibition) of cells. $K_{i,cis}$ represents the inhibition constant for the *cis*-inhibition of OATP1B1 based on the I_{buffer}. $K_{i,trans}$ represents the inhibition constants for the *trans*-inhibition of OATP1B1 based on the intracellular unbound concentration ($I_{cell,u}$). Intracellular unbound fraction (f_T) is set constant (rifampin) or nonlinear (CsA). For CsA showing nonlinear f_T, the intracellular bound concentration ($I_{cell,b}$) is saturable with K_d (dissociation constant), B_{max} (maximum number of binding site for intracellular binding), and A (non-saturable component). Parameters were obtained directly from in vitro experiments or estimated by data fitting (e.g., $K_{i,cis}$ was

DMD Fast Forward. Published on February 28, 2023 as DOI: 10.1124/dmd.122.000970
This article has not been copyedited and formatted. The final version may differ from this version.

experimentally determined by the substrate and inhibitor coincubation, and $K_{i,trans}$ was estimated by the cellular kinetic model analysis, which allowed the calculation of α [$K_{i,cis}$-to-$K_{i,trans}$ ratio]). Reproduced with some modifications from Izumi S, Nozaki Y, Lee W, and Sugiyama Y (2022) Experimental and Modeling Evidence Supporting the Trans-Inhibition Mechanism for Preincubation Time-Dependent, Long-Lasting Inhibition of Organic Anion Transporting Polypeptide 1B1 by Cyclosporine A. *Drug Metab Dispos* **50**:541-551.

Figure 5 Preincubation time-dependent, long-lasting inhibition of OATP1B1 by CsA and rifampin. The inhibitory effects of CsA (A) and rifampin (B) on OATP1B1-mediated uptake of [^{3}H]E_2G were examined in the *cis*-, *trans*-, and *cis*+*trans*-inhibition conditions using OATP1B1-transfected and control HEK293 cells. Detailed assay flow is given in Figure 3. In the *trans*- and *cis*+*trans*-inhibition conditions, CsA and rifampin were preincubated for 10 and 60 (rifampin) or 120 (CsA) minutes. Each symbol represents mean ± SEM (n=3), and solid (*cis*-inhibition), dashed (*trans*-inhibition), and dash-dotted lines (*cis*+*trans*-inhibition) are fitted lines. *Trans*-inhibition of OATP1B1 by CsA (C) and rifampin (D). After preincubation with CsA (for up to 120 minutes) or rifampin (for up to 60 minutes), OATP1B1-mediated uptake of [^{3}H]E_2G was determined in the buffer lacking inhibitors. Observed % of control values (relative to OATP1B1-mediated uptake of [^{3}H]E_2G without inhibitor preincubation) were presented as

DMD Fast Forward. Published on February 28, 2023 as DOI: 10.1124/dmd.122.000970
This article has not been copyedited and formatted. The final version may differ from this version.

closed circles (mean ± SEM, n=3). Solid lines are fitted lines. Long-lasting inhibition of OATP1B1 by CsA (E) and rifampin (F). After preincubation of CsA (for 120 minutes) or rifampin (for 60 minutes) with OATP1B1-transfected and control HEK293 cells, cells were washed and incubated with an inhibitor-free buffer at 37°C. At designated times, buffer was removed, followed by cell washing. Then, OATP1B1-mediated uptake of [^{3}H]E_2G was examined in the buffer lacking inhibitors to see the recovery of OATP1B1 transport function. Each symbol represents observed % of control values (mean ± SEM, n=3). Solid, dashed, and dash-dotted lines are simulated values given by constructed cellular PK model. Reproduced with some modifications from Izumi S, Nozaki Y, Lee W, and Sugiyama Y (2022) Experimental and Modeling Evidence Supporting the Trans-Inhibition Mechanism for Preincubation Time-Dependent, Long-Lasting Inhibition of Organic Anion Transporting Polypeptide 1B1 by Cyclosporine A. *Drug Metab Dispos* **50**:541-551.

Figure 6 Static model-based prediction of DDIs mediated by OATP1B1 inhibition by CsA and rifampin. The R-values of CsA (A) and rifampin (B) for OATP1B1 were calculated according to Method 1 ($R = 1 + I_{u,in,max}/K_{i,cis}$, closed circles), Method 2 ($R = 1 + I_{u,in,max}/K_{i,app,cis+trans}$, open squares), and Method 3 ($R = (1 + I_{u,in,max}/K_{i,cis})\cdot(1 + K_{p,uu,in\ vivo}\cdot I_{u,in,max}/K_{i,trans}$), open triangles) and were compared with clinically observed AUCR values of OATP1B substrate drugs (atorvastatin,

DMD Fast Forward. Published on February 28, 2023 as DOI: 10.1124/dmd.122.000970
This article has not been copyedited and formatted. The final version may differ from this version.

pemafibrate, pitavastatin, rosuvastatin, and valsartan for CsA; pemafibrate, pitavastatin, and rosuvastatin for rifampin). Vertical and horizontal dashed lines represent AUCR of 1.25 and the cut-off for R-values (1.1). R-value calculations and data source for AUCR values are given in Supplemental Table 3.

Table 1 Preincubation-dependent inhibitors for OATP1B1 and OATP1B3

IC_{50} or K_i values determined by substrate and inhibitor coincubation (*cis*-inhibition condition) were compared with those obtained by adding an inhibitor preincubation step (*cis*+*trans*-inhibition condition). Inhibitors that showed 3-fold or greater potentiation after inhibitor preincubation in at least one of the examinations are considered as positive preincubation-dependent inhibitors and listed in this table. All data were obtained from transfected cell systems with HEK293 or HEK293T as host cells. Individual data are given in Supplementary Table 1.

Transporters	Inhibitors[a]	Probe substrate	Preincubation time	Mean IC_{50} or K_i[b]		Mean fold potentiation[b]
				w/o preincubation	w/ preincubation	
			(min)	*(µmol/L)*	*(µmol/L)*	*(fold)*
OATP1B1	CsA	E_2G	30 – 180	0.316 (0.0458 – 0.667)	0.0412 (0.0109 – 0.0983)	10 (3.3 – 27)
		E_1S	30 – 60	0.229 (0.134 – 0.383)	0.0437 (0.0264 – 0.0692)	5.1 (4.8 – 5.5)
		BSP	60	0.252	0.0799	3.2
		Atorvastatin	30 – 60	0.311 (0.112 – 0.47)	0.0263 (0.021 – 0.0319)	13 (4.3 – 22)
		Pitavastatin	30 – 60	0.401 (0.074 – 1.31)	0.0278 (0.013 – 0.048)	10 (3.9 – 27)
		Pemafibrate	30	2.5	0.041	61
		Rosuvastatin	30	0.397 (0.193, 0.60)	0.0631 (0.0312, 0.095)	6.3 (6.2, 6.3)
		Valsartan	60	0.064	0.008	8.0
		CP-I	60	0.163	0.019	8.6
		GCDCA-S	60	0.057	0.009	6.3
		GCDCA-G	60	0.048	0.011	4.4
	AM1	E_2G	30	0.41	0.09	4.4
	Rifampin	E_2G	60 – 180	1.03 (0.74 – 1.20)	0.521 (0.22 – 0.818)	2.3 (1.5 – 3.4)

		Pemafibrate	30	3.62	0.39	9.3
		Pitavastatin	30	4.32	1.25	3.5
		Rosuvastatin	30	3.96	1.05	3.8
	Asunaprevir	E_1S	30	0.17	0.0349	4.9
	Everolimus	E_1S	60	0.61	0.16	3.8
		Rosuvastatin	60	1.58	0.19	8.3
	Nilotinib	E_1S	60	>10	0.235	>42
	Pazopanib	E_2G	60	13.5	2.03	6.7
	Regorafenib	E_1S	60	>10	0.403	>24
	Saquinavir	E_2G	180	3.65	1.03	3.5
	Venetoclax	E_2G	180	>171	0.663	>258
OATP1B3	CsA	E_2G	30 – 180	0.269 (0.14 – 0.505)	0.0797 (0.032 – 0.167)	3.9 (3.0 – 5.1)
		Valsartan	60	0.071	0.022	3.2
		CP-I	60	0.059	0.020	3.0
		GCDCA-S	60	0.094	0.031	3.0
	AM1	E_2G	30	0.191	0.059	3.2
	Saquinavir	E_2G	180	11.0	2.91	3.8
	Venetoclax	E_2G	180	>300	34.5	>8.7

BSP = sulphobromophthalein, CP-I = coproporphyrin I, CsA = cyclosporine A, E_1S = estrone-3-sfulfate, E_2G = estradiol-17β-glucuronide, GCDCA-S = glycochenodeoxycholic acid sulfate, GCDCA-G = glycochenodeoxycholic acid glucuronide.

a: Simeprevir showed the preincubation effect on OATP1B1 and OATP1B3 inhibition, but the fold potentiation was not determined (Furihata et al., 2014).

b: When multiple data source is available, arithmetic mean was calculated for the substrate-inhibitor pair. Range of reported values (or individual values when n=2) are given in the parenthesis.

Table 2 Preincubation-dependent inhibitors for transporters other than OATP1Bs

IC_{50} or K_i values determined by substrate and inhibitor coincubation (*cis*-inhibition condition) were compared with those obtained by adding an inhibitor preincubation step (*cis*+*trans*-inhibition condition). Inhibitors that showed 3-fold or greater potentiation after inhibitor preincubation are considered as positive preincubation-dependent inhibitors and are summarized in this table. The data were obtained from transfected cell systems with HEK293 or MDCKII (for MATE2-K only) as host cells. Individual data are given in Supplementary Table 1.

Transporters	Inhibitors	Probe substrate	Preincubation time	Mean IC_{50} or K_i		Mean fold potentiation
				w/o preincubation	w/ preincubation	
			(min)	*(μmol/L)*	*(μmol/L)*	*(fold)*
OCT1	CsA	Metformin	30	21.6	0.43	50.2
		Fenoterol	30	>20	2.4	>8.3
		Ranitidine	30	>20	4.6	>4.3
		Sumatriptan	30	2.5	0.77	3.2
	Daclatasvir	Metformin	180	0.533	0.0943	5.7
	Irinotecan	Metformin	180	0.121	0.0233	5.2
	Isavuconazole	Metformin	180	5.21	1.75	3.0
	Ledipasvir	Metformin	180	>50	0.196	>255
	Saquinavir	Metformin	180	18.2	4.45	4.1
	Verapamil	Metformin	180	0.459	0.150	3.1
OCT2	Crizotinib	Creatinine	15	1.58	0.347	4.6
		MPP^+	15	16.2	4.58	3.5
	Daclatasvir	Metformin	180	67.8	1.98	34

	Dolutegravir	Metformin	180	23.0	3.71	6.2
	Isavuconazole	Metformin	180	16.8	1.27	13.2
	Ledipasvir	Metformin	180	>200	22.9	>8.7
	Vandetanib	Metformin	180	19.8	4.72	4.2
MATE1	Crizotinib	Creatinine	60	2.16	0.573	3.8
		MPP^+	60	2.66	0.868	3.1
	Imatinib	Creatinine	60	0.466	0.0651	7.2
MATE2-K	Vandetanib	Metformin	180	0.880	0.293	3.0

CsA = cyclosporine A, MPP^+ = 1-methyl-4-phenylpyridinium.

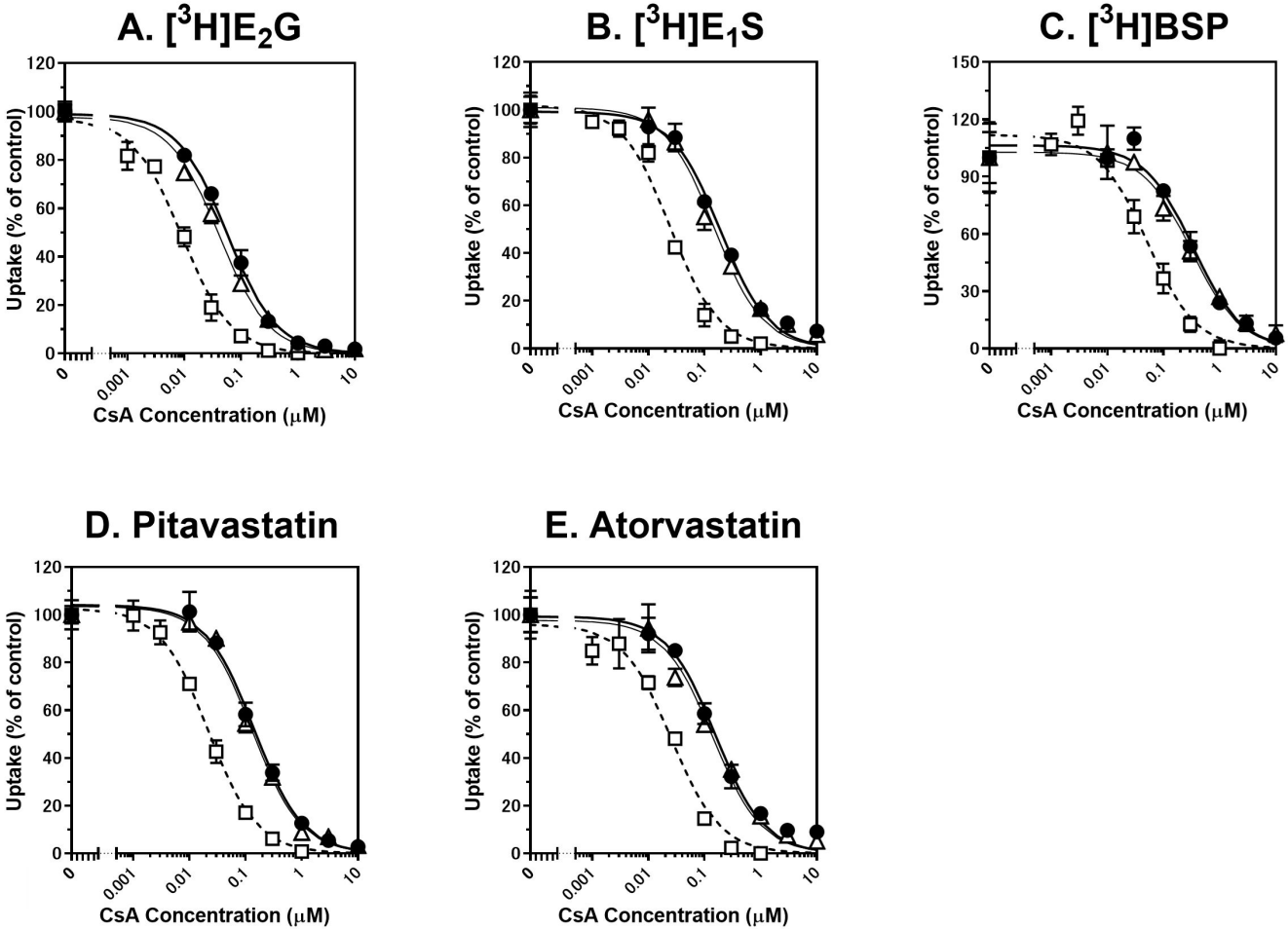
A. [3H]E2G
B. [3H]E1S
C. [3H]BSP
D. Pitavastatin
E. Atorvastatin
Uptake (% of control)
CsA Concentration (μM)
0
0.001
0.01
0.1
1
10
20
30
40
60
80
90
100
120
150

Figure 1

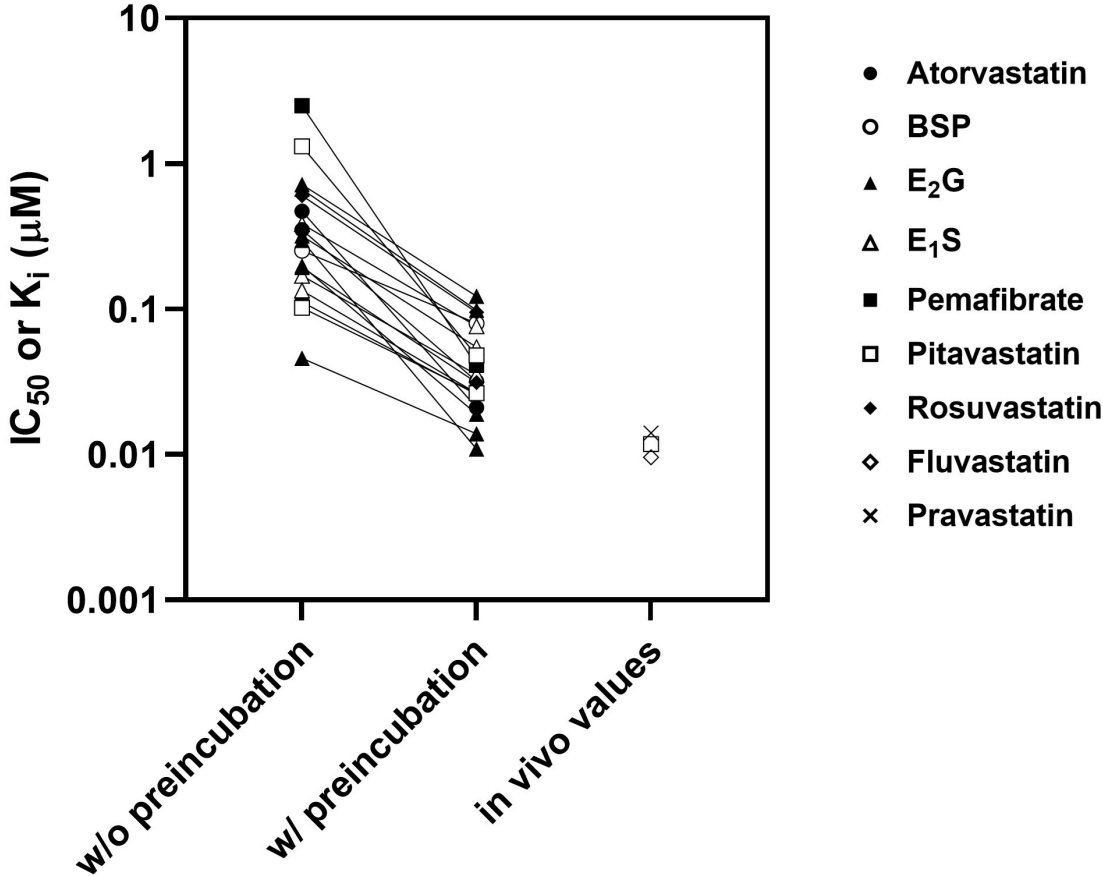
10
1
0.1
0.01
0.001
IC50 or Ki (μM)
w/o preincubation
w/ preincubation
in vivo values
Atorvastatin
BSP
E2G
E1S
Pemafibrate
Pitavastatin
Rosuvastatin
Fluvastatin
Pravastatin

Figure 2

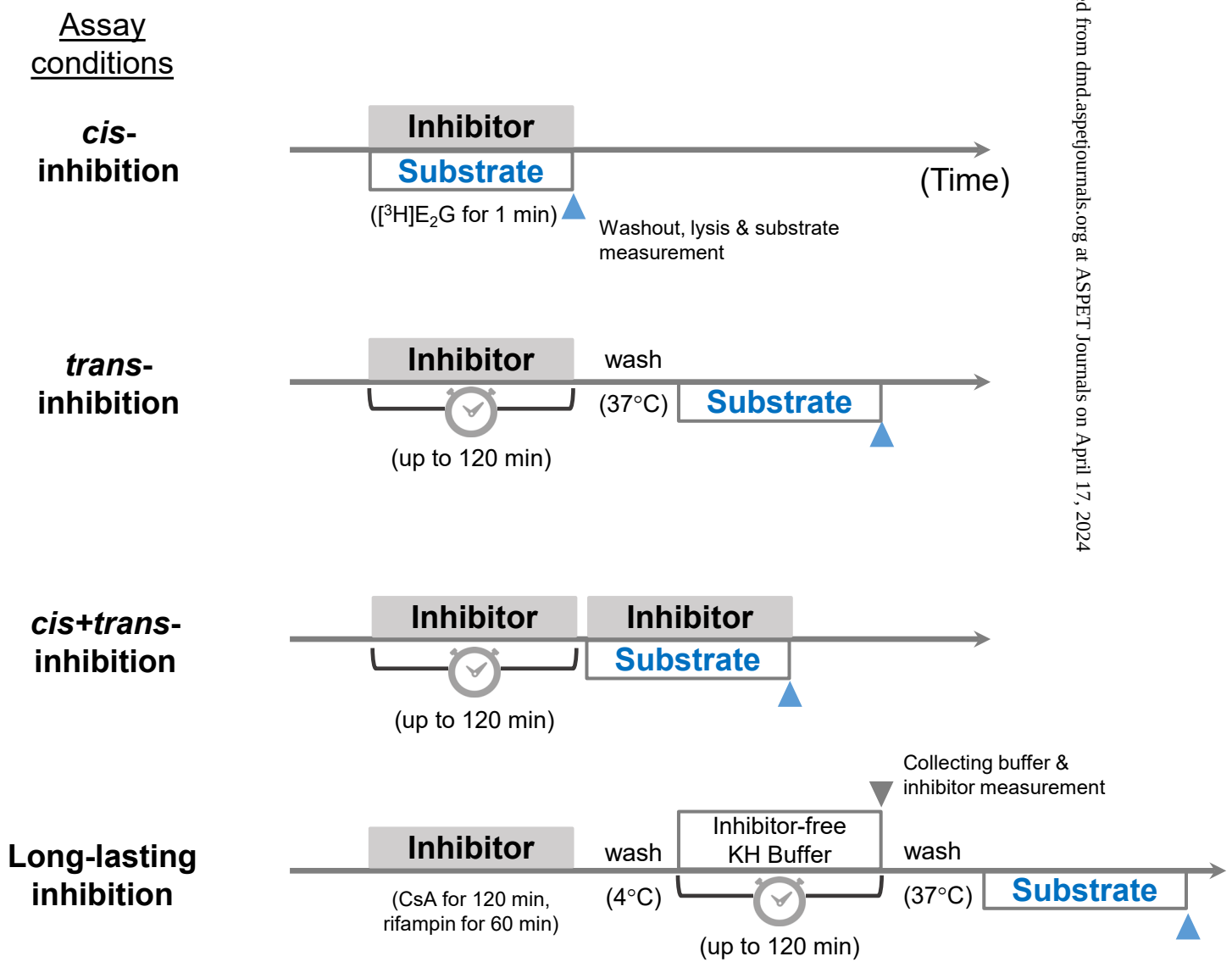

Figure 3

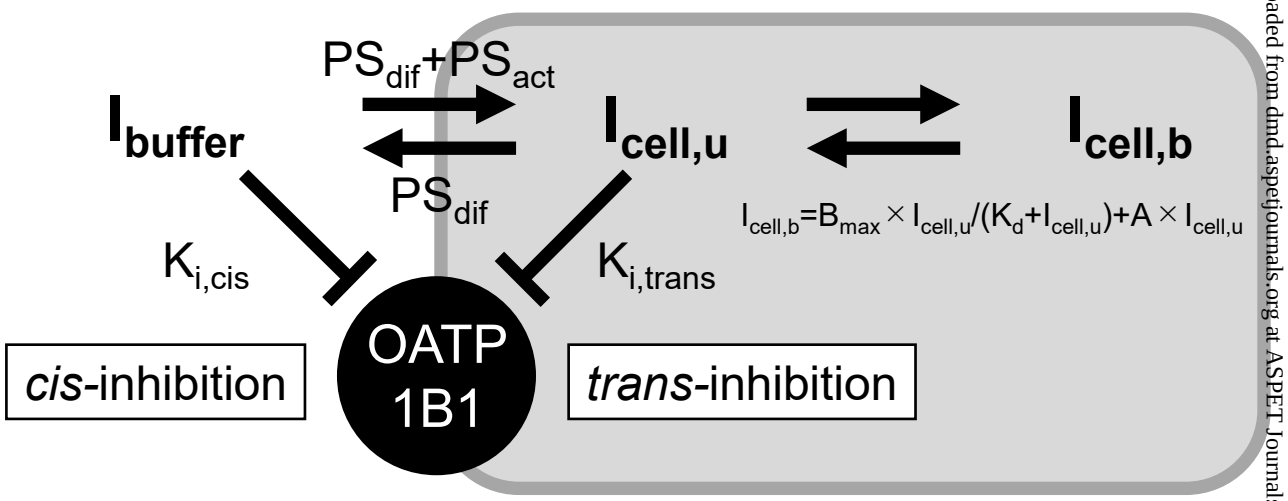

Parameters	Units	Inhibitors	
		CsA	Rifampin
K_d	μM	0.0914	-
B_{max}	μM	326	-
A		362	-
f_T		0.000254	0.0311
PS_{dif}	μl/min/mg protein	51.3	52.5
V_{max}	pmol/min/mg protein	-	25.1
K_m	μM	-	0.382
$K_{p,uu,in\ vitro}$		1	2.25
$K_{i,cis}$	μM	0.297	1.16
$K_{i,trans}$	μM	0.00619	1.56
$K_{i,cis}$-to-$K_{i,trans}$ ratio (α)		48.0	0.744

Figure 4

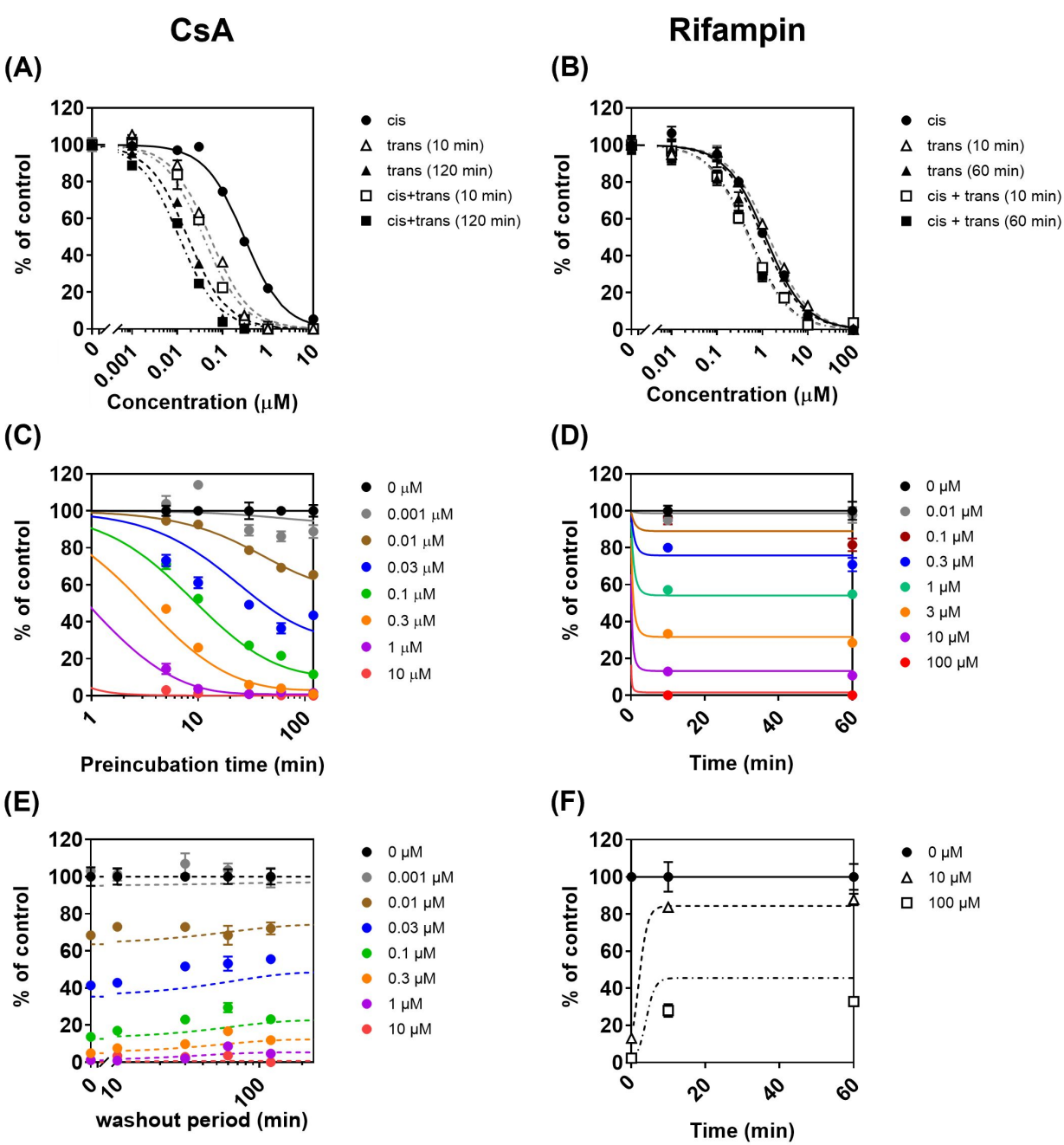

Figure 5

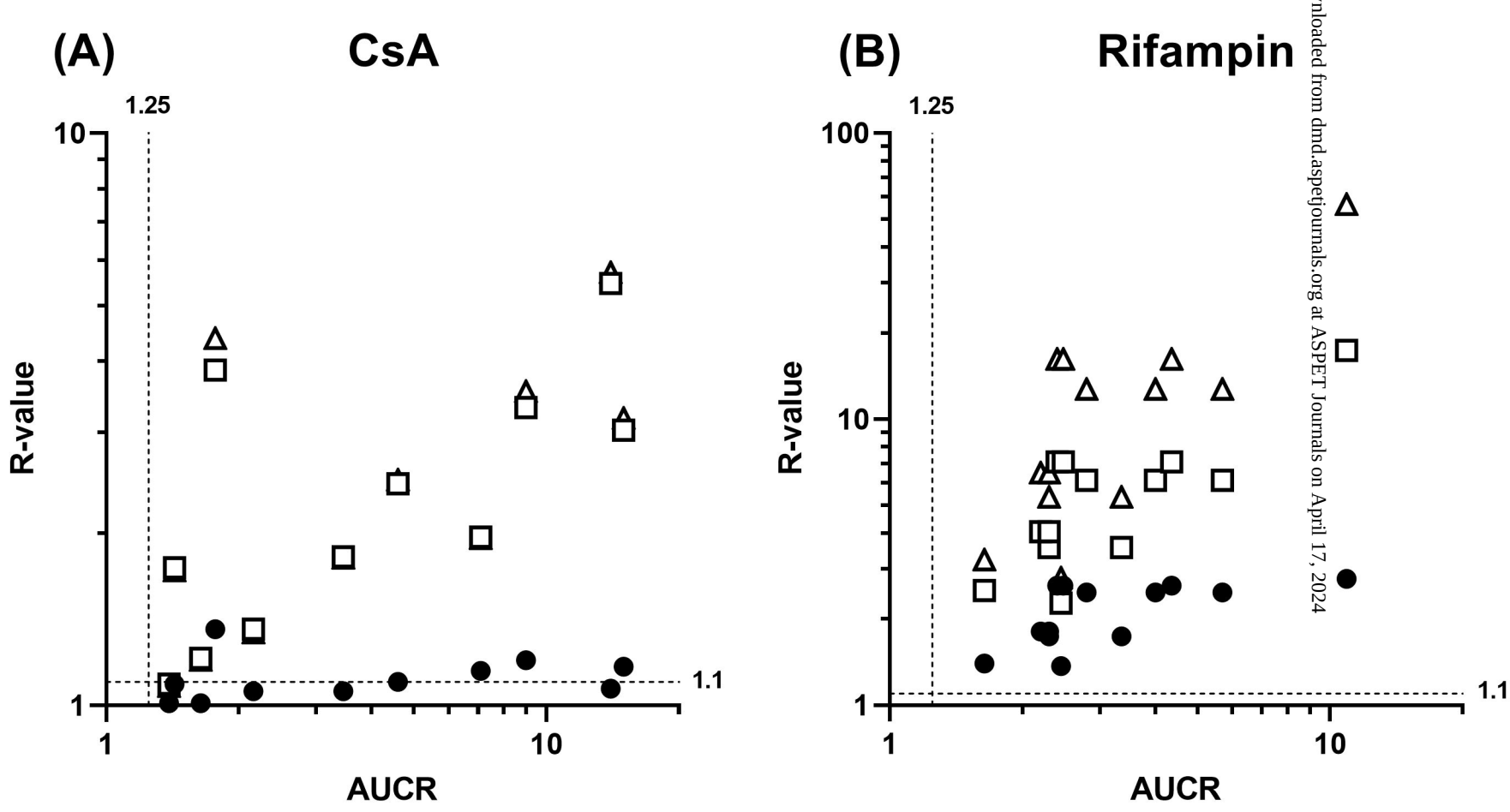

Figure 6

[Title] Preincubation time-dependent, long-lasting inhibition of drug transporters and impact on the prediction of drug-drug interactions

[Authors] Yoshitane Nozaki and Saki Izumi

[Journal] Drug Metabolism and Disposition

Supplemental Table 1 Preincubation effect on the drug transporter inhibition potency observed in transfected cell systems

IC_{50} or K_i values determined by substrate and inhibitor coincubation (*cis*-inhibition condition, w/o preincubation) were compared with those obtained by adding an inhibitor preincubation step (*cis*+*trans*-inhibition condition, w/ preincubation). Inhibitors that showed 3-fold or greater potentiation after inhibitor preincubation are considered as positive preincubation-dependent inhibitors and the fold potentiation values are indicated by boldface in this table.

Transporter	Inhibitor	Probe substrate (conc. in μmol/L)	Host cells	Preincubation time (min)	K_i or IC_{50} value (μmol/L)		Fold potentiation	References
					w/o preincubation	w/ preincubation		
OATP1B1[a,b,c]	CsA	E_2G (0.02-0.06)	HEK293	30	0.198	0.019	**10.4**	(Gertz et al., 2013)
		E_2G	HEK293	30	0.319	0.0548	**5.8**	(Taguchi et al., 2020)
		E_2G (0.1)	HEK293	60	0.0458	0.0139	**3.3**	(Izumi et al., 2015)
		E_2G (1)	HEK293	60	0.37	0.05	**7.4**	(Pahwa et al., 2017)
		E_2G (0.1)	HEK293	120	0.297	0.0109	**27**	(Izumi et al., 2022)
		E_2G (1)	HEK293	180	0.667	0.0983	**6.8**	(Tátrai et al., 2019)
		E_1S	HEK293	30	0.383	0.0692	**5.5**	(Taguchi et al., 2019)
		E_1S	HEK293	30	0.169	0.0354	**4.8**	(Taguchi et al., 2020)
		E_1S (0.01)	HEK293	60	0.134	0.0264	**5.1**	(Izumi et al., 2015)
		BSP (0.01)	HEK293	60	0.252	0.0799	**3.2**	(Izumi et al., 2015)
		Atorvastatin (0.3)	HEK293	30	0.351	0.0319	**11**	(Taguchi et al., 2020)
		Atorvastatin (0.5)	HEK293	60	0.47	0.021	**22**	(Amundsen et al., 2010)
		Atorvastatin (0.1)	HEK293	60	0.112	0.0259	**4.3**	(Izumi et al., 2015)
		Pitavastatin (0.1)	HEK293	30	1.31	0.048	**27**	(Park et al., 2021)
		Pitavastatin (0.5)	HEK293	30	0.119	0.0239	**5.0**	(Taguchi et al., 2020)
		Pitavastatin (0.1)	HEK293	60	0.102	0.0263	**3.9**	(Izumi et al., 2015)
		Pitavastatin (0.1)	HEK293T	60	0.074	0.013	**5.7**	(Mochizuki et al., 2022)
		Pemafibrate (0.1)	HEK293	30	2.5	0.041	**61**	(Park et al., 2021)
		Rosuvastatin (3)	HEK293	30	0.193	0.0312	**6.2**	(Taguchi et al., 2020)
		Rosuvastatin (0.3)	HEK293	30	0.60	0.095	**6.3**	(Park et al., 2021)
		Valsartan (0.5)	HEK293T	60	0.064	0.008	**8.0**	(Mochizuki et al., 2022)

		CP-I (0.05)	HEK293T	60	0.163	0.019	**8.6**	(Mochizuki et al., 2022)
		GCDCA-S (0.5)	HEK293T	60	0.057	0.009	**6.3**	(Mochizuki et al., 2022)
		GCDCA-G (0.5)	HEK293T	60	0.048	0.011	**4.4**	(Mochizuki et al., 2022)
	AM1	E_2G (0.02-0.06)	HEK293	30	0.41	0.09	**4.4**	(Gertz et al., 2013)
	Rifampin	E_2G (1)	HEK293	60	0.74	0.22	**3.4**	(Pahwa et al., 2017)
		E_2G (0.1)	HEK293	60	1.16	0.524	2.2	(Izumi et al., 2022)
		E_2G (1)	HEK293	180	1.20	0.818	1.5	(Tátrai et al., 2019)
		E_1S	HEK293	60	1.50	2.87	0.5	(Taguchi et al., 2019)
		Pemafibrate (0.1)	HEK293	30	3.62	0.39	**9.3**	(Park et al., 2021)
		Pitavastatin (0.1)	HEK293	30	4.32	1.25	**3.5**	(Park et al., 2021)
		Rosvastatin (0.3)	HEK293	30	3.96	1.05	**3.8**	(Park et al., 2021)
	Asunaprevir	E_1S	HEK293	30	0.17	0.0349	**4.9**	(Taguchi et al., 2020)
	Everolimus	E_2G (1)	HEK293	60	0.48	0.23	2.1	(Farasyn et al., 2019)
		E_1S (0.025)	HEK293	60	0.61	0.16	**3.8**	(Farasyn et al., 2019)
		Rosuvastatin (0.020)	HEK293	60	1.58	0.19	**8.3**	(Farasyn et al., 2019)
	Nilotinib	E_1S	HEK293	60	>10	0.235	**>42**	(Taguchi et al., 2020)
	Pazopanib	E_2G	HEK293	60	13.5	2.03	**6.7**	(Taguchi et al., 2019)
		E_1S	HEK293	60	1.42	0.530	2.7	(Taguchi et al., 2019)
	Regorafenib	E_1S	HEK293	60	>10	0.403	**>24**	(Taguchi et al., 2020)
	Saquinavir	E_2G (1)	HEK293	180	3.65	1.03	**3.5**	(Tátrai et al., 2019)
	Venetoclax	E_2G (1)	HEK293	180	>171	0.663	**>258**	(Tátrai et al., 2019)
	Atorvastatin	E_2G (1)	HEK293	180	1.68	0.892	1.9	(Tátrai et al., 2019)
	Dasatinib	E_2G (1)	HEK293	60	4.81	2.33	2.1	(Pahwa et al., 2017)
	Gemfibrozil	E_2G (1)	HEK293	180	32.9	33.7	1.0	(Tátrai et al., 2019)
	6-Hydroxyindole	E_1S (0.0024)	HEK293	24 h	16.7	12.1	1.4	(Masuo et al., 2020)
		E_2G (0.0072)	HEK293	24 h	4.52	5.72	0.8	(Masuo et al., 2020)
	Ruxolitinib	DCF (10)	HEK293	30	14.2	12.1	1.2	(Bruyère et al., 2021)
	Sirolimus	E_2G (1)	HEK293	60	0.64	0.22	2.9	(Farasyn et al., 2019)
		E_1S (0.025)	HEK293	60	0.83	0.65	1.3	(Farasyn et al., 2019)
		Rosuvastatin (0.020)	HEK293	60	0.56	0.32	1.8	(Farasyn et al., 2019)
OATP1B3[b,c]	CsA	E_2G (0.02-0.06)	HEK293	30	0.162	0.032	**5.1**	(Gertz et al., 2013)
		E_2G (1)	HEK293	60	0.14	0.04	**3.5**	(Pahwa et al., 2017)
		E_2G (1)	HEK293	180	0.505	0.167	**3.0**	(Tátrai et al., 2019)
		Pitavastatin (0.1)	HEK293T	60	0.047	0.025	1.9	(Mochizuki et al., 2022)
		Valsartan (0.5)	HEK293T	60	0.071	0.022	**3.2**	(Mochizuki et al., 2022)

		CP-I (0.05)	HEK293T	60	0.059	0.020	**3.0**	(Mochizuki et al., 2022)
		GCDCA-S (0.5)	HEK293T	60	0.094	0.031	**3.0**	(Mochizuki et al., 2022)
	AM1	E_2G (0.02-0.06)	HEK293	30	0.191	0.059	**3.2**	(Gertz et al., 2013)
	Saquinavir	E_2G (1)	HEK293	180	11.0	2.91	**3.8**	(Tátrai et al., 2019)
	Venetoclax	E_2G (1)	HEK293	180	>300	34.5	**>8.7**	(Tátrai et al., 2019)
	Rifampin	E_2G (1)	HEK293	60	0.26	0.11	2.4	(Pahwa et al., 2017)
		E_2G (1)	HEK293	180	3.67	2.13	1.7	(Tátrai et al., 2019)
	Atorvastatin	E_2G (1)	HEK293	180	0.710	0.314	2.3	(Tátrai et al., 2019)
	Dasatinib	E_2G (1)	HEK293	60	5.76	2.75	2.1	(Pahwa et al., 2017)
	Everolimus	CCK-8 (1)	HEK293	60	0.51	0.19	2.7	(Farasyn et al., 2019)
	Gemfibrozil	E_2G (1)	HEK293	180	246	366	0.7	(Tátrai et al., 2019)
	Sirolimus	CCK-8 (1)	HEK293	60	0.97	0.36	2.7	(Farasyn et al., 2019)
OAT1[d]	Benzbromarone	E_2G (1)	HEK293	180	2.68	1.47	1.8	(Tátrai et al., 2019)
	Bumetanide	E_2G (1)	HEK293	180	50.8	42.6	1.2	(Tátrai et al., 2019)
	Diclofenac	E_2G (1)	HEK293	180	8.64	6.89	1.3	(Tátrai et al., 2019)
	Furosemide	E_2G (1)	HEK293	180	45.5	31.7	1.4	(Tátrai et al., 2019)
	Gemfibrozil	E_2G (1)	HEK293	180	12.7	24.7	0.5	(Tátrai et al., 2019)
	Pravastatin	E_2G (1)	HEK293	180	>300	>300	NC	(Tátrai et al., 2019)
	Probenecid	E_2G (1)	HEK293	180	14.4	10.5	1.4	(Tátrai et al., 2019)
	Rifampin	E_2G (1)	HEK293	180	>100	>100	NC	(Tátrai et al., 2019)
	Saquinavir	E_2G (1)	HEK293	180	>100	>100	NC	(Tátrai et al., 2019)
	Valsartan	E_2G (1)	HEK293	180	22.7	16.2	1.4	(Tátrai et al., 2019)
OAT3[d]	Benzbromarone	E_2G (1)	HEK293	180	5.76	3.82	1.5	(Tátrai et al., 2019)
	Furosemide	E_2G (1)	HEK293	180	5.98	8.28	0.7	(Tátrai et al., 2019)
	Valsartan	E_2G (1)	HEK293	180	3.57	2.26	1.6	(Tátrai et al., 2019)
	Probenecid	E_2G (1)	HEK293	180	3.01	1.91	1.6	(Tátrai et al., 2019)
	Diclofenac	E_2G (1)	HEK293	180	3.10	7.24	0.4	(Tátrai et al., 2019)
	Bumetanide	E_2G (1)	HEK293	180	3.35	2.53	1.3	(Tátrai et al., 2019)
	Gemfibrozil	E_2G (1)	HEK293	180	7.46	6.14	1.2	(Tátrai et al., 2019)
	Rifampin	E_2G (1)	HEK293	180	>100	>100	NC	(Tátrai et al., 2019)
	Saquinavir	E_2G (1)	HEK293	180	>100	>100	NC	(Tátrai et al., 2019)
	Pravastatin	E_2G (1)	HEK293	180	>300	>300	NC	(Tátrai et al., 2019)
	Ruxolitinib	6-CF (10)	HEK293	30	3.1	2.9	1.1	(Bruyère et al., 2021)
OCT1	CsA	Metformin (2)	HEK293	30	21.6	0.43	**50.2**	(Panfen et al., 2019)
		Fenoterol (1)	HEK293	30	>20	2.4	**>8.3**	(Panfen et al., 2019)

		Ranitidine (1)	HEK293	30	>20	4.6	**>4.3**	(Panfen et al., 2019)
		Sumatriptan (1)	HEK293	30	2.5	0.77	**3.2**	(Panfen et al., 2019)
		MPP^+ (1)	HEK293	30	>20	16.1	>1.2	(Panfen et al., 2019)
		TEA (2)	HEK293	30	>20	12.1	>1.7	(Panfen et al., 2019)
		Cycloguanil (1)	HEK293	30	0.32	0.15	2.1	(Panfen et al., 2019)
	Daclatasvir	Metformin (10)	HEK293	180	0.533	0.0943	**5.7**	(Tátrai et al., 2019)
	Irinotecan	Metformin (10)	HEK293	180	0.121	0.0233	**5.2**	(Tátrai et al., 2019)
	Isavuconazole	Metformin (10)	HEK293	180	5.21	1.75	**3.0**	(Tátrai et al., 2019)
	Ledipasvir	Metformin (10)	HEK293	180	>50	0.196	**>255**	(Tátrai et al., 2019)
	Saquinavir	Metformin (10)	HEK293	180	18.2	4.45	**4.1**	(Tátrai et al., 2019)
	Verapamil	Metformin (10)	HEK293	180	0.459	0.150	**3.1**	(Tátrai et al., 2019)
	Abacavir	Metformin (10)	HEK293	180	99.9	112	0.9	(Tátrai et al., 2019)
	Amisulpride	Metformin (10)	HEK293	180	25.3	15.7	1.6	(Tátrai et al., 2019)
	Cetirizine	Metformin (10)	HEK293	180	91.5	51.3	1.8	(Tátrai et al., 2019)
	Cimetidine	Metformin (10)	HEK293	180	150	87.6	1.7	(Tátrai et al., 2019)
	Dolutegravir	Metformin (10)	HEK293	180	>300	>300	NC	(Tátrai et al., 2019)
	Pyrimethamine	Metformin (2)	HEK293	30	1.8	1.3	1.4	(Panfen et al., 2019)
	Quinidine	Metformin (2)	HEK293	30	7.7	4.5	1.7	(Panfen et al., 2019)
	Ranolazine	Metformin (10)	HEK293	180	66.9	49.5	1.4	(Tátrai et al., 2019)
	Ritonavir	Metformin (2)	HEK293	30	2.2	1.1	2.0	(Panfen et al., 2019)
	Trimethoprim	Metformin (2)	HEK293	30	9.6	9.2	1.0	(Panfen et al., 2019)
		Metformin (10)	HEK293	180	27.8	20.6	1.3	(Tátrai et al., 2019)
	Vandetanib	Metformin (10)	HEK293	180	5.22	1.94	2.7	(Tátrai et al., 2019)
OCT2[d]	Crizotinib	Creatinine (2.6)	HEK293	15	1.58	0.347	**4.6**	(Arakawa et al., 2017)
		MPP^+ (0.0025)	HEK293	15	16.2	4.58	**3.5**	(Arakawa et al., 2017)
	Daclatasvir	Metformin (10)	HEK293	180	67.8	1.98	**34**	(Tátrai et al., 2019)
	Dolutegravir	Metformin (10)	HEK293	180	23.0	3.71	**6.2**	(Tátrai et al., 2019)
	Isavuconazole	Metformin (10)	HEK293	180	16.8	1.27	**13.2**	(Tátrai et al., 2019)
	Ledipasvir	Metformin (10)	HEK293	180	>200	22.9	**>8.7**	(Tátrai et al., 2019)
	Vandetanib	Metformin (10)	HEK293	180	19.8	4.72	**4.2**	(Tátrai et al., 2019)
	Abacavir	Metformin (10)	HEK293	180	>300	>300	NC	(Tátrai et al., 2019)
	Amisulpride	Metformin (10)	HEK293	180	150	127	1.2	(Tátrai et al., 2019)
	Cetirizine	Metformin (10)	HEK293	180	113	73.1	1.5	(Tátrai et al., 2019)
	Cimetidine	Metformin (10)	HEK293	180	>300	>300	NC	(Tátrai et al., 2019)
	Irinotecan	Metformin (10)	HEK293	180	57.3	27.0	2.1	(Tátrai et al., 2019)

	Ranolazine	Metformin (10)	HEK293	180	235	218	1.1	(Tátrai et al., 2019)
	Ruxolitinib	4-Di-ASP (10)	HEK293	30	1.2	1.7	0.7	(Bruyère et al., 2021)
	Saquinavir	Metformin (10)	HEK293	180	>100	>100	NC	(Tátrai et al., 2019)
	Trimethoprim	Metformin (10)	HEK293	180	98.3	77.0	1.3	(Tátrai et al., 2019)
	Verapamil	Metformin (10)	HEK293	180	36.2	19.5	1.9	(Tátrai et al., 2019)
MATE1	Crizotinib	Creatinine (2.5)	HEK293	60	2.16	0.573	**3.8**	(Omote et al., 2018)
		MPP^+ (0.0025)	HEK293	60	2.66	0.868	**3.1**	(Omote et al., 2018)
	Imatinib	Creatinine (2.5)	HEK293	60	0.466	0.0651	**7.2**	(Omote et al., 2018)
	Cimetidine	Metformin (10)	MDCKII	180	4.32	3.41	1.3	(Tátrai et al., 2019)
	Famotidine	Metformin (10)	MDCKII	180	1.63	1.45	1.1	(Tátrai et al., 2019)
	Isavuconazole	Metformin (10)	MDCKII	180	7.16	4.67	1.5	(Tátrai et al., 2019)
	Ondansetron	Metformin (10)	MDCKII	180	0.0913	0.0580	1.6	(Tátrai et al., 2019)
	Pyrimethamine	Metformin (10)	MDCKII	180	0.03614	0.01927	1.9	(Tátrai et al., 2019)
	Ranitidine	Metformin (10)	MDCKII	180	13.1	19.6	0.7	(Tátrai et al., 2019)
	Ruxolitinib	TEA (40)	HEK293	30	2.5	2.3	1.1	(Bruyère et al., 2021)
	Trimethoprim	Metformin (10)	MDCKII	180	14.1	8.05	1.8	(Tátrai et al., 2019)
	Vandetanib	Metformin (10)	MDCKII	180	0.794	0.438	1.8	(Tátrai et al., 2019)
MATE2-K	Vandetanib	Metformin (10)	MDCKII	180	0.880	0.293	**3.0**	(Tátrai et al., 2019)
	Cimetidine	Metformin (10)	MDCKII	180	7.54	10.1	0.7	(Tátrai et al., 2019)
	Famotidine	Metformin (10)	MDCKII	180	54.1	31.2	1.7	(Tátrai et al., 2019)
	Isavuconazole	Metformin (10)	MDCKII	180	20.8	15.1	1.4	(Tátrai et al., 2019)
	Ondansetron	Metformin (10)	MDCKII	180	0.354	0.342	1.0	(Tátrai et al., 2019)
	Pyrimethamine	Metformin (10)	MDCKII	180	0.106	0.0507	2.1	(Tátrai et al., 2019)
	Ranitidine	Metformin (10)	MDCKII	180	18.8	42.9	0.4	(Tátrai et al., 2019)
	Ruxolitinib	TEA (40)	HEK293	30	1.1	1.0	1.1	(Bruyère et al., 2021)
	Trimethoprim	Metformin (10)	MDCKII	180	1.13	1.06	1.1	(Tátrai et al., 2019)

BSP = sulphobromophthalein, CCK-8 = cholecystokinin octapeptide, 6-CF = 6-carboxyfluorescein, CP-I = coproporphyrin I, CsA = cyclosporine A, DCF = dichlorofluorescein, 4-Di-ASP = 4-(4-dimethylamino)styryl)-N-methylpyridinium iodide, E_1S = estrone-3-sfulfate, E_2G = estradiol-17β-glucuronide, GCDCA-S = glycochenodeoxycholic acid sulfate, GCDCA-G = glycochenodeoxycholic acid glucuronide, MPP^+ = 1-methyl-4-phenylpyridinium, NC = not calculated, TEA = tetraethylammonium.

a: Following compounds did not show the preincubation effect on OATP1B1 inhibition potency in vitro: rifamycin SV, sildenafil, clarithromycin, erythromycin, telmisartan, glibenclamide, ketoconazole (Shitara et al., 2012; Shitara et al., 2013).

b: Tacrolimus did not show the preincubation effect on OATP1B1 or OATP1B3 inhibition potency (Shitara et al., 2012).

c: Simeprevir showed the preincubation effect on OATP1B1 and OATP1B3 inhibition potency, but the fold potentiation was not calculated (Furihata et al., 2014).

d: CsA did not show the preincubation effect on OAT1, OAT3, or OCT2 inhibition potency (Panfen et al., 2019).

[References]

Amundsen R, Christensen H, Zabihyan B, and Asberg A (2010) Cyclosporine A, but not tacrolimus, shows relevant inhibition of organic anion-transporting protein 1B1-mediated transport of atorvastatin. *Drug Metab Dispos* **38:**1499-1504.

Arakawa H, Omote S, and Tamai I (2017) Inhibitory Effect of Crizotinib on Creatinine Uptake by Renal Secretory Transporter OCT2. *J Pharm Sci* **106:**2899-2903.

Bruyère A, Le Vée M, Jouan E, Molez S, Nies AT, and Fardel O (2021) Differential in vitro interactions of the Janus kinase inhibitor ruxolitinib with human SLC drug transporters. *Xenobiotica* **51:**467-478.

Farasyn T, Crowe A, Hatley O, Neuhoff S, Alam K, Kanyo J, Lam TT, Ding K, and Yue W (2019) Preincubation With Everolimus and Sirolimus Reduces Organic Anion-Transporting Polypeptide (OATP)1B1- and 1B3-Mediated Transport Independently of mTOR Kinase Inhibition: Implication in Assessing OATP1B1- and OATP1B3-Mediated Drug-Drug Interactions. *J Pharm Sci* **108:**3443-3456.

Furihata T, Matsumoto S, Fu Z, Tsubota A, Sun Y, Matsumoto S, Kobayashi K, and Chiba K (2014) Different interaction profiles of direct-acting anti-hepatitis C virus agents with human organic anion transporting polypeptides. *Antimicrob Agents Chemother* **58:**4555-4564.

Gertz M, Cartwright CM, Hobbs MJ, Kenworthy KE, Rowland M, Houston JB, and Galetin A (2013) Cyclosporine inhibition of hepatic and intestinal CYP3A4, uptake and efflux transporters: application of PBPK modeling in the assessment of drug-drug interaction potential. *Pharm Res* **30:**761-780.

Izumi S, Nozaki Y, Lee W, and Sugiyama Y (2022) Experimental and Modeling Evidence Supporting the Trans-Inhibition Mechanism for Preincubation Time-Dependent, Long-Lasting Inhibition of Organic Anion Transporting Polypeptide 1B1 by Cyclosporine A. *Drug Metab Dispos* **50:**541-551.

Izumi S, Nozaki Y, Maeda K, Komori T, Takenaka O, Kusuhara H, and Sugiyama Y (2015) Investigation of the impact of substrate selection on in vitro organic anion transporting polypeptide 1B1 inhibition profiles for the prediction of drug-drug interactions. *Drug Metab Dispos* **43:**235-247.

Masuo Y, Fujita KI, Mishiro K, Seba N, Kogi T, Okumura H, Matsumoto N, Kunishima M, and Kato Y (2020) 6-Hydroxyindole is an endogenous long-lasting OATP1B1 inhibitor elevated in renal failure patients. *Drug Metab Pharmacokinet* **35:**555-562.

Mochizuki T, Zamek-Gliszczynski MJ, Yoshida K, Mao J, Taskar K, Hirabayashi H, Chu X, Lai Y, Takashima T, Rockich K, Yamaura Y, Fujiwara K, Mizuno T, Maeda K, Furihata K, Sugiyama Y, and Kusuhara H (2022) Effect of Cyclosporin A and Impact of Dose Staggering on OATP1B1/1B3 Endogenous Substrates and Drug Probes for Assessing Clinical Drug Interactions. *Clin Pharmacol Ther* **111:**1315-1323.

Omote S, Matsuoka N, Arakawa H, Nakanishi T, and Tamai I (2018) Effect of tyrosine kinase inhibitors on renal handling of creatinine by MATE1. *Sci Rep* **8:**9237.

Pahwa S, Alam K, Crowe A, Farasyn T, Neuhoff S, Hatley O, Ding K, and Yue W (2017) Pretreatment With Rifampicin and Tyrosine Kinase Inhibitor Dasatinib Potentiates the Inhibitory Effects Toward OATP1B1- and OATP1B3-Mediated Transport. *J Pharm Sci* **106:**2123-2135.

Panfen E, Chen W, Zhang Y, Sinz M, Marathe P, Gan J, and Shen H (2019) Enhanced and Persistent Inhibition of Organic Cation Transporter 1 Activity by Preincubation of Cyclosporine A. *Drug Metab Dispos* **47:**1352-1360.

Park JE, Shitara Y, Lee W, Morita S, Sahi J, Toshimoto K, and Sugiyama Y (2021) Improved Prediction of the Drug-Drug Interactions of Pemafibrate Caused by Cyclosporine A and Rifampicin via PBPK Modeling: Consideration of the Albumin-Mediated Hepatic Uptake of Pemafibrate and Inhibition Constants With Preincubation Against OATP1B. *J Pharm Sci* **110:**517-528.

Shitara Y, Takeuchi K, and Horie T (2013) Long-lasting inhibitory effects of saquinavir and ritonavir on OATP1B1-mediated uptake. *J Pharm Sci* **102:**3427-3435.

Shitara Y, Takeuchi K, Nagamatsu Y, Wada S, Sugiyama Y, and Horie T (2012) Long-lasting inhibitory effects of cyclosporin A, but not tacrolimus, on OATP1B1- and OATP1B3-mediated uptake. *Drug Metab Pharmacokinet* **27:**368-378.

Taguchi T, Masuo Y, Futatsugi A, and Kato Y (2020) Static Model-Based Assessment of OATP1B1-Mediated Drug Interactions with Preincubation-Dependent Inhibitors Based on Inactivation and Recovery Kinetics. *Drug Metab Dispos* **48:**750-758.

Taguchi T, Masuo Y, Sakai Y, and Kato Y (2019) Short-lasting inhibition of hepatic uptake transporter OATP1B1 by tyrosine kinase inhibitor pazopanib. *Drug Metab Pharmacokinet* **34:**372-379.

Tátrai P, Schweigler P, Poller B, Domange N, de Wilde R, Hanna I, Gáborik Z, and Huth F (2019) A Systematic In Vitro Investigation of the Inhibitor Preincubation Effect on Multiple Classes of Clinically Relevant Transporters. *Drug Metab Dispos* **47:**768-778.

[Title] Preincubation time-dependent, long-lasting inhibition of drug transporters and impact on the prediction of drug-drug interactions

[Authors] Yoshitane Nozaki and Saki Izumi

[Journal] Drug Metabolism and Disposition

Supplemental Table 2 Preincubation effect on the drug transporter inhibition potency observed in human and monkey hepatocytes

IC_{50} or K_i values determined by substrate and inhibitor coincubation (*cis*-inhibition condition, w/o preincubation) were compared with those obtained by adding an inhibitor preincubation step (*cis*+*trans*-inhibition condition, w/ preincubation). Inhibitors that showed 3-fold or greater potentiation after inhibitor preincubation are considered as positive preincubation-dependent inhibitors and the fold potentiation values are indicated by boldface in this table.

Transporter	Inhibitor	Probe substrate (conc. in μmol/L)	In vitro systems	Preincubation time	K_i or IC_{50} value (μmol/L)		Fold potentiation	References
				(min)	w/o preincubation	w/ preincubation		
OATP1Bs	Everolimus	Pitavastatin (1)	SCHH	60	5.16	0.50	**10**	(Farasyn et al., 2019)
		Rosuvastatin (0.5)	SCHH	60	1.81	0.64	2.8	(Farasyn et al., 2019)
		CCK-8 (1)	SCHH	60	1.89	0.53	**3.6**	(Farasyn et al., 2019)
	Sirolimus	CCK-8 (1)	SCHH	60	2.72	0.36	**7.6**	(Farasyn et al., 2019)
		Rosuvastatin (0.5)	SCHH	60	1.90	0.77	2.5	(Farasyn et al., 2019)
		Pitavastatin (1)	SCHH	60	0.93	0.87	1.1	(Farasyn et al., 2019)
	Rifampin	CP-I (0.03)	Plated HH	60	0.73	0.30	2.4	(Barnett et al., 2018)
		Rosuvastatin (2)	Plated HH	60	1	1	1.0	(Barnett et al., 2018)
		Rosuvastatin (1)	Plated MH	60	1.14	0.54	2.1	(Ufuk et al., 2018)
		Pitavastatin (0.3)	Plated MH	60	3.80	2.98	1.3	(Ufuk et al., 2018)
	CsA	Rosuvastatin (1)	Plated MH	60	0.72	0.10	**7.2**	(Ufuk et al., 2018)
		Pitavastatin (0.3)	Plated MH	60	0.78	0.21	**3.7**	(Ufuk et al., 2018)
	Rifamycin SV	Pitavastatin (0.3)	Plated MH	60	6.17	4.30	1.4	(Ufuk et al., 2018)

CCK-8 = cholecystokinin octapeptide, CP-I = coproporphyrin I, HH = human hepatocytes, MH = monkey hepatocytes, SCHH = sandwich-cultured human hepatocytes.

[References]

Barnett S, Ogungbenro K, Ménochet K, Shen H, Lai Y, Humphreys WG, and Galetin A (2018) Gaining Mechanistic Insight Into Coproporphyrin I as Endogenous Biomarker for OATP1B-Mediated Drug-Drug Interactions Using Population Pharmacokinetic Modeling and Simulation. *Clin Pharmacol Ther* **104:**564-574.

Farasyn T, Crowe A, Hatley O, Neuhoff S, Alam K, Kanyo J, Lam TT, Ding K, and Yue W (2019) Preincubation With Everolimus and Sirolimus Reduces Organic Anion-Transporting Polypeptide

(OATP)1B1- and 1B3-Mediated Transport Independently of mTOR Kinase Inhibition: Implication in Assessing OATP1B1- and OATP1B3-Mediated Drug-Drug Interactions. *J Pharm Sci* **108:**3443-3456.

Ufuk A, Kosa RE, Gao H, Bi YA, Modi S, Gates D, Rodrigues AD, Tremaine LM, Varma MVS, Houston JB, and Galetin A (2018) In Vitro-In Vivo Extrapolation of OATP1B-Mediated Drug-Drug Interactions in Cynomolgus Monkey. *J Pharmacol Exp Ther* **365:**688-699.

[Title] Preincubation time-dependent, long-lasting inhibition of drug transporters and impact on the prediction of drug-drug interactions

[Authors] Yoshitane Nozaki and Saki Izumi

[Journal] Drug Metabolism and Disposition

Supplemental Table 3 R-value calculations to predict OATP1B1-mediated DDIs with CsA and rifampin by static models

According to Method 1 ($R = 1 + I_{u,in,max}/K_{i,cis}$), Method 2 ($R = 1 + I_{u,in,max}/K_{i,app,cis+trans}$), and Method 3 ($R = (1 + I_{u,in,max}/K_{i,cis})\cdot(1 + K_{p,uu,in\ vivo}\cdot I_{u,in,max}/K_{i,trans})$), R-values of CsA and rifampin were calculated for each of the OATP1B1 substrate drugs and compared with AUCR values overserved in vivo. When calculated R-values are equal to or greater than the regulatory cut-off value (1.1), they are indicated by boldface in this table.

Inhibitor	Dose (mg)	$K_{p,uu,in\ vivo}$[a]	$K_{p,uu,in\ vitro}$[b]	Substrate	$K_{i,app,cis+trans}$ (μmol/L)	$K_{i,cis}$ (μmol/L)	$K_{i,trans}$[c] (μmol/L)	R-value[d]			AUCR	References
								Method 1	Method 2	Method 3		
CsA	175	1	1	Atorvastatin	0.0263	0.311	0.0312	**1.17**	**3.03**	**3.18**	15	(Yoshida et al., 2012)
	200							**1.20**	**3.32**	**3.54**	9.0	(Yoshida et al., 2012)
	600			Pemafibrate	0.041	2.5	0.0424	1.07	**5.47**	**5.71**	14.0	(Park et al., 2021)
	20			Pitavastatin	0.0278	0.401	0.0319	1.01	**1.21**	**1.20**	1.64	(Mochizuki et al., 2022)
	75							1.06	**1.82**	**1.81**	3.46	(Mochizuki et al., 2022)
	131							**1.10**	**2.44**	**2.48**	4.6	(Yoshida et al., 2012)
	20			Rosuvastatin	0.0631	0.397	0.0869	1.01	1.09	1.08	1.39	(Mochizuki et al., 2022)
	75							1.06	**1.36**	**1.34**	2.16	(Mochizuki et al., 2022)
	200							**1.15**	**1.97**	**1.96**	7.1	(Yoshida et al., 2012)
	20			Valsartan	0.008	0.064	0.0103	1.09	**1.74**	**1.72**	1.43	(Mochizuki et al., 2022)
	75							**1.36**	**3.86**	**4.38**	1.77	(Mochizuki et al., 2022)
Rifampin	600	3.3	2.25	Pemafibrate	0.39	3.62	1.09	**2.77**	**17.41**	**56.43**	10.9	(Park et al., 2021)
	150			Pitavastatin	1.25	4.32	5.10	**1.37**	**2.28**	**2.79**	2.45	(Mori et al., 2020)
	300							**1.74**	**3.56**	**5.34**	2.3	(Takehara et al., 2018)
	300							**1.74**	**3.56**	**5.34**	3.36	(Mori et al., 2020)
	600							**2.48**	**6.12**	**12.75**	5.7	(Prueksaritanont et al., 2014)
	600							**2.48**	**6.12**	**12.75**	2.8	(Takehara et al., 2018)
	600							**2.48**	**6.12**	**12.75**	4.01	(Mori et al., 2020)
	150			Rosuvastatin	1.05	3.96	4.07	**1.40**	**2.52**	**3.23**	1.64	(Mori et al., 2020)
	300							**1.81**	**4.05**	**6.50**	2.2	(Takehara et al., 2018)
	300							**1.81**	**4.05**	**6.50**	2.30	(Mori et al., 2020)

600	**2.62**	**7.10**	**16.20**	4.37	(Prueksaritanont et al., 2014)
600	**2.62**	**7.10**	**16.20**	2.4	(Takehara et al., 2018)
600	**2.62**	**7.10**	**16.20**	2.48	(Mori et al., 2020)

AUCR = area under the plasma concentration-time curve ratio.

a: $K_{p,uu,in\ vivo}$ was assumed to be unity for CsA. Reported value (3.3) was used for rifampin (Chu et al., 2015).

b: $K_{p,uu,in\ vitro}$ values determined in our previous study (Izumi et al., 2022) (Figure 4) were used in this preliminary analysis.

c:$K_{i,trans}$ values were calculated according to Eq. 9 using $K_{i,app,cis+trans}$, $K_{i,cis}$, and $K_{p,uu,in\ vitro}$ values that were determined or estimated in vitro.

d: $I_{u,in,max}$ of CsA reported to be 5.9 nmol/L at 20 mg and 22.9 nmol/L at 75 mg (Mochizuki et al., 2022) were used for calculating R-values. The $I_{u,in,max}$ of CsA at 131 mg or higher was estimated from that at 75 mg (22.9 nmol/L) assuming linear PK. $I_{u,in,max}$ of 6.4 μmol/L at 600 mg (Yoshida et al., 2012) was used for rifampin, and linear PK was assumed for estimating the $I_{u,in,max}$ at lower dose levels (150 and 300 mg).

[References]

Chu X, Shih SJ, Shaw R, Hentze H, Chan GH, Owens K, Wang S, Cai X, Newton D, Castro-Perez J, Salituro G, Palamanda J, Fernandis A, Ng CK, Liaw A, Savage MJ, and Evers R (2015) Evaluation of cynomolgus monkeys for the identification of endogenous biomarkers for hepatic transporter inhibition and as a translatable model to predict pharmacokinetic interactions with statins in humans. *Drug Metab Dispos* **43:**851-863.

Izumi S, Nozaki Y, Lee W, and Sugiyama Y (2022) Experimental and Modeling Evidence Supporting the Trans-Inhibition Mechanism for Preincubation Time-Dependent, Long-Lasting Inhibition of Organic Anion Transporting Polypeptide 1B1 by Cyclosporine A. *Drug Metab Dispos* **50:**541-551.

Mochizuki T, Zamek-Gliszczynski MJ, Yoshida K, Mao J, Taskar K, Hirabayashi H, Chu X, Lai Y, Takashima T, Rockich K, Yamaura Y, Fujiwara K, Mizuno T, Maeda K, Furihata K, Sugiyama Y, and Kusuhara H (2022) Effect of Cyclosporin A and Impact of Dose Staggering on OATP1B1/1B3 Endogenous Substrates and Drug Probes for Assessing Clinical Drug Interactions. *Clin Pharmacol Ther* **111:**1315-1323.

Mori D, Kimoto E, Rago B, Kondo Y, King-Ahmad A, Ramanathan R, Wood LS, Johnson JG, Le VH, Vourvahis M, David Rodrigues A, Muto C, Furihata K, Sugiyama Y, and Kusuhara H (2020) Dose-Dependent Inhibition of OATP1B by Rifampicin in Healthy Volunteers: Comprehensive Evaluation of Candidate Biomarkers and OATP1B Probe Drugs. *Clin Pharmacol Ther* **107:**1004-1013.

Park JE, Shitara Y, Lee W, Morita S, Sahi J, Toshimoto K, and Sugiyama Y (2021) Improved Prediction of the Drug-Drug Interactions of Pemafibrate Caused by Cyclosporine A and Rifampicin via PBPK Modeling: Consideration of the Albumin-Mediated Hepatic Uptake of Pemafibrate and Inhibition Constants With Preincubation Against OATP1B. *J Pharm Sci* **110:**517-528.

Prueksaritanont T, Chu X, Evers R, Klopfer SO, Caro L, Kothare PA, Dempsey C, Rasmussen S, Houle R, Chan G, Cai X, Valesky R, Fraser IP, and Stoch SA (2014) Pitavastatin is a more sensitive and selective organic anion-transporting polypeptide 1B clinical probe than rosuvastatin. *Br J Clin Pharmacol* **78:**587-598.

Takehara I, Yoshikado T, Ishigame K, Mori D, Furihata KI, Watanabe N, Ando O, Maeda K, Sugiyama Y, and Kusuhara H (2018) Comparative Study of the Dose-Dependence of OATP1B

Inhibition by Rifampicin Using Probe Drugs and Endogenous Substrates in Healthy Volunteers. *Pharm Res* **35:**138.

Yoshida K, Maeda K, and Sugiyama Y (2012) Transporter-mediated drug--drug interactions involving OATP substrates: predictions based on in vitro inhibition studies. *Clin Pharmacol Ther* **91:**1053-1064.